Academic year 2019-2020

Levelized cost minimization of hydrogen in a combined renewable hydrogen and electricity supply on neighborhood scale

Full Name of Student: *Edrick Orvin Victor Tromp*

Core Provider: *Hanze University of Applied Sciences, Zernikeplein 7, 9747AS, Groningen, The Netherlands*

Specialization: *Hanze University of Applied Sciences, Zernikeplein 7, 9747AS, Groningen, The Netherlands*

Host Organization: *Energy Transition Centre, Zernikeplein 17, 9747AA, Groningen, The Netherlands*

Academic Supervisor: *Dr. Evert Jan Hengeveld*

Submission Date: *15 February 2021*

Declaration of originality

By this letter, I declare that I have written this thesis completely by myself, and that I have used no other sources or resources than the ones mentioned.

The sources used, have been stated in accordance with the EUREC Project Guidelines. I have indicated all quotes and citations that were literally taken from publications, or that were in close accordance with the meaning of those publications, as such. Moreover, I have not handed in an essay, paper or thesis with similar contents elsewhere. All sources and other resources used are stated in the bibliography.

In case of proof that the essay, paper or thesis has not been constructed in accordance with this declaration, the School of Engineering considers the essay, paper or thesis as negligence or as a deliberate act that has been aimed at making correct judgment of the candidate's expertise, insights and skills impossible.

In case of plagiarism the examiner has the right to exclude the student from any further participation in the particular assignment, and also to exclude the student from further participation in the MSc program at the School of Engineering of Hanze University of Applied Sciences, Groningen. The study results obtained in the course will be declared null and void in case of plagiarism (also see Article 14 of the Teaching and Examination Regulations).

Name: Edrick Orvin Victor Tromp

Place: Oranjestad, Aruba

Date: 15 February 2021

Signature: 

Acknowledgement

I would like to thank my company supervisor Jan Bekkering for all his help and guidance to finish this project. Without him it would not have been possible. I would also like to thank my first supervisor Evert Jan Hengeveld for the advice and feedback he provided to improve the work.

Summary

Renewable energy systems are a crucial technological development needed to combat climate change. This thesis covers the design and implementation of a mathematical optimization model, which calculates the lowest cost of hydrogen for certain renewable energy system configurations. The output of the model can be used to indicate possible costs of hydrogen, for different energy systems configurations and end uses such a mobility and heating.

The research was set up to answer the following research question: Which component sizes lead to the lowest levelized cost of hydrogen for different energy system configurations and meets the various demands (hydrogen for heating, hydrogen for mobility, electricity use) and emission limits at all times? The energy system is assumed to possibly consist of the following variable size components: wind energy generators, solar energy generators, grey grid electricity, battery system, electrolyser, heating hydrogen storage, mobility hydrogen storage and fixed size components: gas receiving station, refueling compressor and hydrogen refueling station.

The model was formulated as a linear programming problem. A hydrogen project being developed in Hoogeveen, The Netherlands, was used as a case study to implement the model. In order to analyze the effects of the used energy system components, various renewable energy system configurations were optimized using the model.

Analysis of the operational performance of one of these scenarios was consistent, showing no strange trends, thus indicating possible real-life operation. After analyzing the results of the optimized energy system configurations, the following observations where apparent: All of the systems prefer grid electricity uptake over renewable electricity generation for a majority of electricity supply if no constraints are applied to the system. The grid electricity uptake percentage of variable costs is also the highest cost component for these scenarios. Putting an emission constraint on the system increases the cost. Hydrogen storage lowers the cost when used in emission constrained systems but at high capacities. Storage also becomes the highest percentage of variable cost for these scenarios. Solar scenarios lead to the highest costs followed by wind and combined wind and solar have the lowest costs.

The lowest costs calculated by the model for hydrogen for heating are 21.3 €/kg H_2 with no emission constraint and 28€/kg H_2 with an emission constraint. The component sizes for this hydrogen for heating system are power generation equivalence of 1.071 60 kW wind turbine units, 6723.8 MWh grid uptake, 7473 kWh heating storage capacity and 182.8 kW electrolyser capacity for the no emission constraint scenario. For the emission constraint scenario, the component sizes are power generation equivalence of 3.179 60 kW wind turbine units, 2214.7 MWh grid uptake, 177.2 kWh battery capacity, 165.9 kW electrolyser capacity and 52928 kWh hydrogen heating storage capacity. For mobility this would be 30.37 and 34.32 €/kg H_2. The mobility hydrogen system component sizes follow the same tendencies as the heating hydrogen system, which are mentioned above.

Previous literature gives costs of hydrogen production ranging 0.94 to 20 €/kg for heating and ranging 3.2-29.7 €/kg for mobility. The costs determined by this model are on the higher end of these ranges and do not seem extreme, and with costs on the lower range being deemed cost competitive, indicates significant cost reductions being needed before hydrogen becomes competitive with conventional technologies.

Contents

1 Introduction

One of the biggest challenges concerning the prosperity of humanity in the near future are the effects of anthropogenic climate change. In a report by the Intergovernmental Panel on Climate Change (IPCC) the increase in both the global land and ocean temperatures, increase in the global sea level, decrease of the ocean pH, decreasing ice mass on both land and sea and increase in the global Green House Gas (GHG) concentrations is described [1]. While these climate changes took place, anthropogenic CO_2 emissions have also been increasing at record setting pace, with around 50% of the anthropogenic CO_2 emissions between 1750 and 2011 occurring in the last 40 years [1]. This does not seem to be slowing down, with the emissions being higher in the last decade (2000-2010) despite more climate change mitigation policies being put into place. Some of the main causes for these emissions are the global population and economic growth that is driven by burning fossil fuels (78% of the CO_2 emissions between 1970 and 2010 is attributed to fossil fuel combustion) [1]. The report concludes that it is extremely likely that anthropogenic GHG emissions and other drivers are a primary cause of the warming in the 20th century. To stop these negative global impacts, various international mitigation and adaptation agreements such as the Kyoto Protocol and Paris Agreement have been signed. One of the most important areas where these agreements can drive change is technological development.

The Netherlands being a signatory state of the Paris Agreement is also driven to make an impact in the technological development. One of the technologies which is thought of potentially being promising is hydrogen. Some advantages of hydrogen are: the nonpolluting nature and easy accessibility of its feedstock (water), the possibility to produce it only using green energy (electrolysis using renewable energy) and a wide range of possible applications such as heating, mobility, energy storage and as a chemical feedstock. But it also has its disadvantages such as: difficult storage properties (low volumetric density, high pressure needed for compression and very low temperatures needed for liquefaction) These properties make usage more difficult due to the conditions and complementary technologies needed. Among the different hydrogen projects being developed is a neighborhood in the municipality of Hoogeveen that uses hydrogen (renewable non GHG emitting fuel) to meet its heating demand instead of natural gas (fossil fuel). However, future energy systems require more decarbonization than only heating demand. Including mobility demand, electricity demand and multiple renewable resources would constitute a more complete energy system that could be deployed in the future. Ultimately the emissions of these energy systems should be limited within certain ranges. In order to determine the viability of an energy system cost is often the parameter analyzed. Minimizing the cost is the goal of these analysis and this is done often using optimization methods. In order to see where the optimization of such an energy system (using the Hoogeveen project as a case study) fits in the framework of energy/hydrogen supply chain models, a literature review was done.

1.1 Literature review

Li et al. presented a comprehensive review on the design of hydrogen supply chains (HSCs) in the context of mobility [2]. This review was analyzed to see if there is a knowledge gap and a breakdown is given of the conclusions on the state of HSC design in regards to mobility. Following this, an analysis was done on some general energy system optimization models. This is due to the consideration of multiple demands, which are of other supply chains (electricity demand, heating demand and mobility demand).

Hydrogen supply chain for mobility review

The review by Li et al. [2] classified various papers regarding HSCs for mobility according to the following points:

1. Model type: refers to the optimization method that was used, which included linear programming (LP), mixed integer linear programming (MILP) and dynamic programming (DP). These optimization models can afterwards be grouped into the following categories:
   Energy system optimization models (ESOM): models that use LP/MILP to meet the energy service demands at the lowest cost. Can be used for different spatial scales. Usually, multi-layered model which includes the whole HSC (various feedstocks, hydrogen production technologies and transportation modes, each of these can be considered a layer). If there are competing end use technologies, composition of the HSC is endogenously optimized (value determined by the model).
   Geographically explicit optimization models (GEOM): have similarities with ESOM but are oriented towards the deployment of hydrogen infrastructures. This can be understood as the model giving an actual result of where and how the technology will be implemented on a map.
   Refueling station locating models: Similar to GEOM but specifically formulated for hydrogen refueling stations and usually used for smaller scales (cities/regions).
2. Research object: refers to whether the model is a multi-layer or mono-layer model. Most of the work reviewed is of the multi-layer type, which makes sense since this is one of the strengths of the optimization methods used.
3. Spatial scale: refers to the spatial scale of the model, distinguishing between international, national, regional and urban models.
4. Whether the mathematical formulation of the model is present in the paper: Important for analyzing the mathematics of the modelling approach used.

Following the classification of all the references, Li et al. [2] filtered the papers for further analysis based on the following criteria:

1. The entire HSC should be considered by the model (all layers of the supply chain).
2. Objective functions, decision variables and constraints definitions should be included.
3. The mathematical formulation of the model should be given in detail.

This resulted in 32 papers meeting the criteria. After this the citational relationship between the papers was determined, resulting in the work by Almansoori and Shah [3] being the seminal paper in this area of literature. Much of the further work in this topic made modifications to this work. The modifications are classified into four categories which are:

1. Implementing a multi-objective optimization
2. Implementing a multi-period optimization
3. Introducing uncertainty
4. Integration with other supply chains

Looking at all the classifications done by Li et al. [2], there is no previous work done which uses LP, is multi-layered, uses an urban spatial scale and has integration with other supply chains. So, there is a knowledge gap.

Some modelling concepts to be considered

Next, the review considers decisions and the planning time horizon of previous work. It is stated that planning decisions in terms of planning the time horizon can be divided into three levels: strategic, tactical and operational. The decisions regarding HSCs are strategic. Li et al. [2] define strategic decisions as: Strategic decisions refer to the location of facilities, the capacity of these facilities, geographical customer areas to serve, as well as the transportation means (ships, trucks, railway, etc.) to use. In other words, they are decisions that must be made immediately and are long-term decisions. This is usually for the lifetime of a project which translates to years or decades. These strategic decisions can be directly translated to the decision variables which are used in the optimization model. In the context of the energy system being considered, these decisions would be related to the components of the energy system that would need to be deployed. Also related to the planning time horizon is whether the model is a mono-period or multi-period model. Multi-period models have benefits such as incorporating the change expected in certain model inputs/parameters throughout the years (such as changing demand or incorporating learning rates for technologies). This consideration is probably more valid on projects where it is expected that expansion will take place, so more regional, national and international spatial resolution rather than the urban resolution of this project. This is another aspect that needs to be taken into consideration for the energy system, whether there is expected expansion taking place.

The HSC performance measures are the next topic which are considered. These are divided into:

1. Cost
2. Environmental impact
3. Safety
4. Multi-objective combination of any of the above

The performance measure is the criteria that the objective function is formulated on. Thus, it is of utmost importance to any optimization, setting the characteristic that the optimization is judged on. For cost this would be the lowest cost system, for environmental impact it could be the system with the lowest emissions and for safety it could be the system with the least amount of accidents/faults/best reliability.

Uncertainty in the model is the next topic reviewed. Where uncertainty is defined as one of the differences between the amount of required information and available information to execute a task [2]. This basically means that the model is not all encompassing and thus does not have all the perfect information to predict the future, which means the output is inherently uncertain. Uncertainty will not be considered in this work.

Selected hydrogen-based energy system optimization models

The springboard in HSC research began with the paper by Almansoori et al. [3]. The paper was published in 2006. This paper incorporated all components along the HSC into one framework, which was something that was not considered beforehand. Some simplifying assumptions taken in this work are that the HSC operates at steady-state (demand is time-invariant) and that the HSC output is a snapshot (no migration pathway from existing infrastructure to the developed one). Examples of some of the modifications made on this work include Almansoori et al. [4] taking away the steady-state/snapshot element by incorporating feedstock/demand evolution in the formulation, Almansoori et al. [5] and Nunes et al. [6] included demand uncertainty in the modelling, Han et al. [7] integrating other supply chains into the framework, Samsatli et al. [8] and Welder et al. [9] putting more detail into spatio-temporal aspects of the modelling and Li et al. [10] integrating HSC network design model with hydrogen fuel station planning models to obtain a novel

formulation. All these network models are on a larger spatial scale (national/regional), unlike the system considered for this paper.

Non hydrogen-based energy system optimization models

Clack et al. [11] employed LP for the design and optimization of an electric power system which included variable generators, conventional generators, transmission and storage. Continental USA is used as a case study. Two LP programming approaches are employed, one using load matching (minimization of the deviation of electric load requirements) and the other minimized cost as the objective function. The model output is the electric system configuration which best meets LP formulation. This optimization considers only electricity and is on a large spatial scale.

Fripp [12] describes the Switch power system plannning tool, which is a linear optimisation model that chooses the optimal investment (to lower GHG emissions at the lowest cost and maintain a reliable supply of power) in renewable and conventional generators over a large spatial scale and over a multi-decade period (multi-period model). With the modelling being different, but the output similar to Clack et al. This is also a large spatial scale optimization.

Lambert et al. [13] describe the HOMER micropower system modelling tool, which can be used to design and compare various micropower systems for various applications. The spatial scale of these HOMER optimized systems is more similar with the Hoogeveen case study compared to the previously considered work. HOMER finds the system configuration that minimizes the total net present cost, while satisfying the user defined constraints. A key difference from the other work and this work is that the user can exogenously (determined outside the model) input the search space in terms of decisions variables, which then gives the total configurations HOMER optimizes for. This happens endogenously for the other work, with the LP obtaining the optimum, which does not have to be a configuration precisely defined by the user (this is indirectly done by the constraints used in the formulation). It is desired that optimizations to be performed are endogenous in nature, thus not similar to what was done in this work.

De La Cruz et al. [14] developed a model for the optimal scheduling of a grid-connected microgrid with different intermittent renewable energy generation. The model is formulated as an MILP mathematical problem. The objective function of the model is to find the minimum costs of operating the microgrid, while satisfying the user defined constraints. This paper is slightly different from the others reviewed, as it is on a smaller spatial scale, but gives insight into how a smaller system can be modelled to derive useful information regarding its operation instead of large scale results regarding its design. The components sizes for this work are already defined, which is not known for the energy system being considered. The optimisation is also more based on operational performance instead of component deployment.

Knowledge gap

Looking at the previous work on HSCs and some other energy system optimisation models, there are many similarities. Because they all use linear optimisation, the problem formulations are all similar, only with the model components and input changing (hydrogen based for HSC and electricity based for some other power system models). Most of the work has been done considering larger spatial scale and also some using multi-period time horizons. However there was no work found which uses LP, is multi-layered, uses an urban spatial scale and has integration with other supply chains. This thesis addresses this knowledge gap. The effects of different variables (system components) and inputs (demand and weather data profiles) on the levelised cost of hydrogen (LCOH) looks to be analysed by performing optimisations of different system configurations. For the classifications used for these type of models, this one can be identified as a model which is mono-objective in

terms of cost, mono-period in its time period, multi-layered (from feedstock to demand being met), urban in its spatial scale, and attempts to integrate multiple supply chains (electricity from wind/PV/grid, heating and mobility demand) using LP.

1.2 Research questions

The energy system is assumed to possibly consist of the following variable size components: wind energy generators, solar energy generators, grey grid electricity, battery system, electrolyser, heating hydrogen storage, mobility hydrogen storage and fixed size components: gas receiving station, refueling compressor and hydrogen refueling station. Emissions of the energy system must also comply with decarbonization goals. In line with the indicated knowledge gap a main research was formulated as: Which component sizes lead to the lowest levelized cost of hydrogen (LCOH) for different energy system configurations and meets the various demands (hydrogen for heating, hydrogen for mobility, electricity use) and emission limits at all times?

In order to answer the main question, the following sub-questions are formulated:

-How should the individual components of the system be modelled?

-How should the model be formulated in an LP form?

-What is the data input and parameter values needed for the modelling and where can these be obtained?

Summarizing path forward for the research

By answering this research question, this work aims to fill the knowledge gap present in energy system supply chain models with regards to a model which uses LP, is multi-layered, uses an urban spatial scale, and has integration with other supply chains. This is done by incorporating scenarios which include the electricity demand, hydrogen demand for mobility and hydrogen demand for heating. The renewable electricity generation will be considered for both wind and solar energy using a weather data-oriented approach. The components considered of the system are mentioned above. The modelling approach being used will be LP. The Hoogeveen hydrogen neighborhood project will be used as a case study. Especially the mobility demand is of interest due to expected development/growth in regards to hydrogen mobility. Possible advantages of incorporating hydrogen mobility in such a setting is an important part of this research. The developed model will be used to calculate the minimized LCOH for different energy system configurations. Capping the emissions by constraining grid energy uptake will also give insight into how future costs could develop. The model output will give project developers insight into what kind of costs can be expected by these types of projects for multiple system configurations. Such information can help drive forward the development of these projects, which will have a positive effect in the fight against climate change.

1.3 Outline

The rest of the report consists of the following sections. Chapter 2 is the methodology used to build the model. Chapter 3 gives the mathematical formulation and the parameter selection of the developed model. Chapter 4 gives the model output results and discusses these. Finally, chapter 5 gives the conclusions and recommendations.

2 Methodology

The next section covers the method used to design the model which will be optimized. First an overview is given of the entire system being modelled, followed by detailed descriptions of each individual component of the system. Finally, an overview is given of the scenarios which will be performed.

2.1 Energy system

The model is build using the Hoogeveen hydrogen project as a case study. This is a project of a neighborhood consisting of 80 houses. The heating demand of the 80 houses will be met using hydrogen. Previous work [15] developed an optimization model using LP to calculate the minimized LCOH for this case study. This work expands the case study by looking at mobility demand based on hydrogen and electricity demand as well. The electricity demand and mobility demand of 80 houses are thus also considered. Figure 1 shows the proposed energy system model. It is assumed to be a local decentralized supply chain with a grid connection to insure energy supply at all times. Electricity can be provided by solar, wind and from the grid i.e., grey grid electricity. The intermediary variable size components of the system consist of a battery system, electrolyser, hydrogen storage for mobility and hydrogen storage for heating, and fixed size components gas receiving station, compressor and refueling station. In Figure 1 the system boundaries are indicated. The timescale used for the modelling is on an hourly basis, thus supply and demand need to be matched on an hourly basis. All of the variables considered are also calculated for the hourly timescale. Electricity can be bought from the grid, but the grid components itself are not considered.

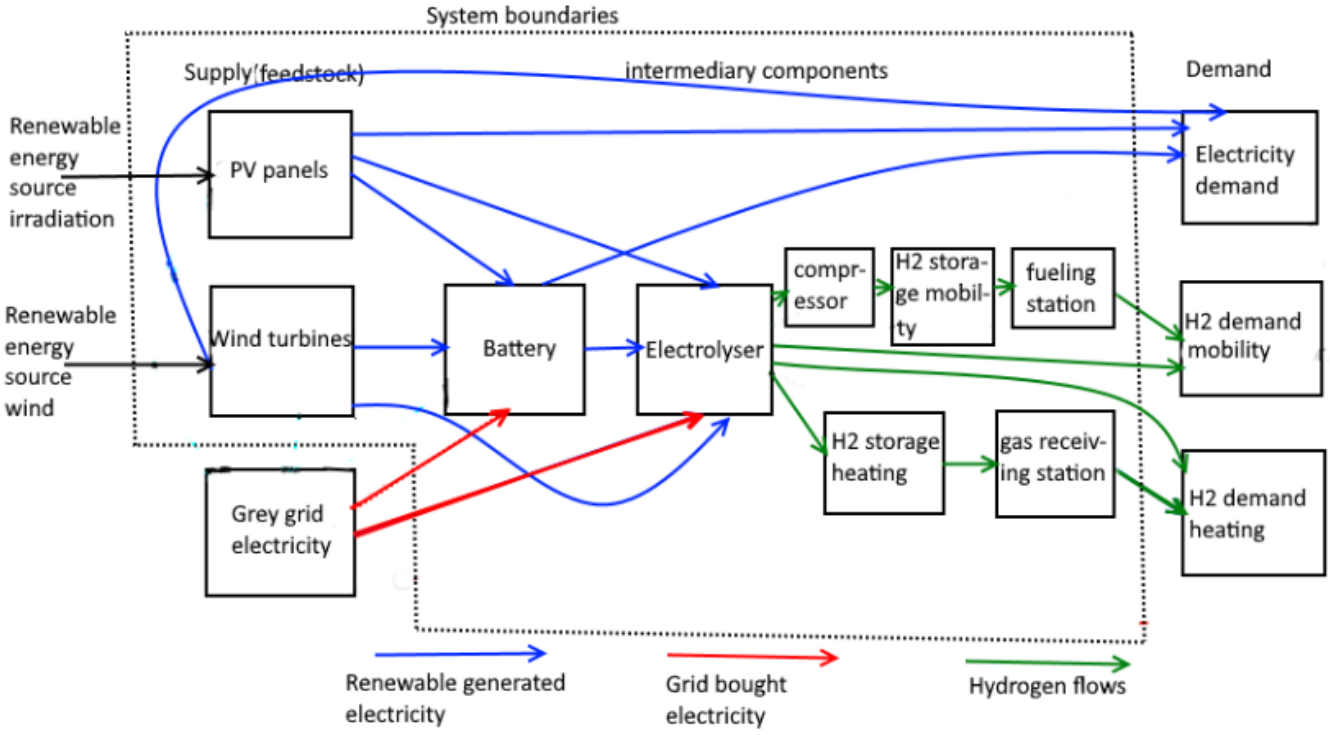

Figure 1: Energy system being modelled in this paper.

Demands

The hourly demands that have to be met are also shown as the output. These demand profiles are shown graphically in Figure 2 for a whole year and for a week. The demand profiles are given for one year, while the model developed considers multiyear timescales**.** The same yearly pattern is thus recycled over all the years. The details of the demand profiles are covered later in this chapter.

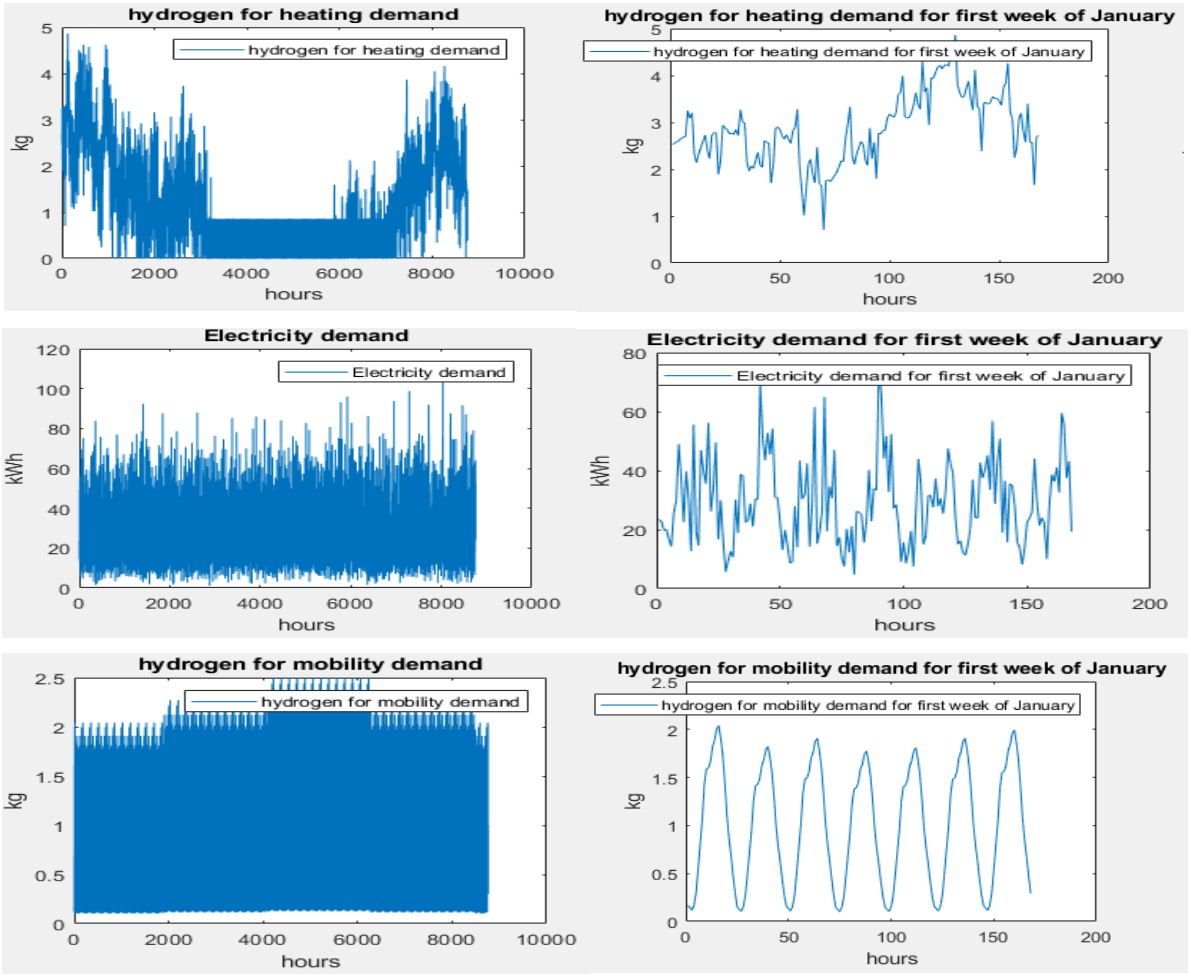

Figure 2: All of the demand profiles used, yearly and weekly resolution. The heating and electricity demand profiles were provided by EnTranCe.

The optimization determines the size of the renewable energy generators and intermediary components needed to meet the demands for every hour of operation at the lowest net present cost.

Energy conversions

Wind and solar energy are converted into electricity which can be used to meet electricity demand directly, be stored in the battery system for times when renewable production is lacking or be converted into hydrogen via water electrolysis directly. Hydrogen can also be produced by using energy stored in the battery system. Grid electricity can be used to produce hydrogen if there is no renewable production and the battery system is empty. The grid cannot serve electricity demand of the homes directly, because the houses are considered to be net zero energy homes. This entails that the production of renewable electricity has to at least equalize the electricity demand. This demand is not matched by the grid directly. From the output of the electrolyser to the final demand the hydrogen also flows through the fixed size components such as the gas receiving station, compressor and refueling station.

Input output model structure

Figure 3 gives the model input and outputs. The left side of this figure considers the models input, which are the sections covered in this chapter. These numbers are used in the linear optimization model which will be defined in the following chapter. The output is the results calculated by the optimization with some postprocessing involved and is given in the results chapter.

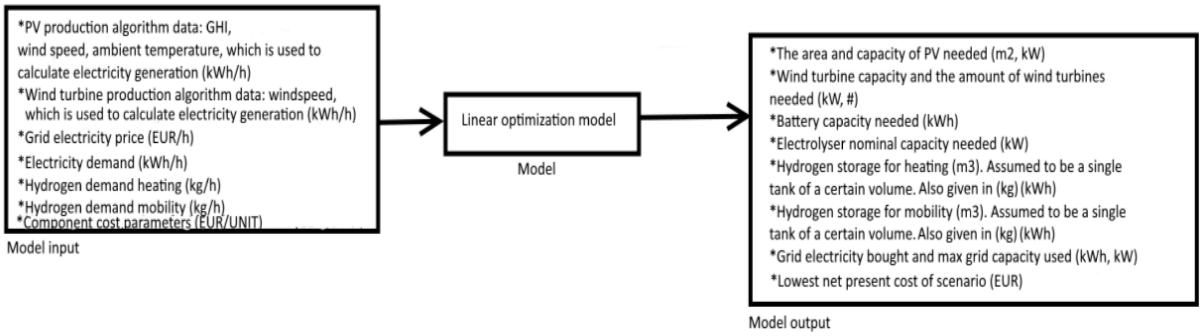

Figure 3: Input and output of the linear optimization model.

Certain modelling aspects not included

The electrical infrastructure costs are not included because these are assumed to be dependent on geometric distances between the components that are not known. The hydrogen transportation network costs are approximated by using project specific cost figures [16] [17]. However, the model does track the flows between the components and if the geometric data is available, these costs can be included afterwards by taking the largest flows that goes in between the components and multiplying them by the parameters of these transmission/transport technologies. The influence that these factors would have on the calculated costs would be additional capital expenditures (CAPEX) and operation and maintenance (O&M) cost of these components.

Another factor that is not tracked precisely is the effect of possible hydrogen storage/network/refueling station electricity use on the emission constraint. These costs are included in the fixed costs used to calculate the net present cost (NPC) contribution of these technologies, but the electricity use is not precisely tracked and delivered by PV, wind turbines or grid as there is no connection between these blocks and the fixed size component blocks. However, if these connections are established and the constraint applied, the net result would be a scenario meeting the constraint. Thus, it is assumed that the electricity use of not connected components meets the sustainability requirements.

Ideal scenario optimization

Optimization of the energy system given by Figure 1 complying with emission constraints gives the configuration needed to meet all demands required by an energy system in a sustainable future using the considered technologies. Integration of all these options would show possible synergies between technologies and demand profiles, which could be used to lower system costs. Unfortunately, due to the complete system having the most number of variables, the hourly resolution used for modelling and limited hardware availability, this optimization was not possible. However, optimizations involving less components and demands are valuable. They would not indicate possible synergy effects between multiple demands, but the influence of components on system cost will still be apparent. The work was carried forward implementing optimizations of increasing complexity, until the computational time became excessive.

2.2 Solar energy

The objective of this component of the model is to determine the amount of installed PV needed to meet demands at the lowest cost. For this, weather data is needed as input into a PV system power production algorithm. The weather data used in this case is Hoogeveen weather data taken from the Royal Netherlands Meteorological Institute (KNMI). The right side of Figure 4 shows the data being used over one day to have good resolution. The variability is immediately apparent. Data from multiple years is used as input into the power production algorithm which is the equations from [14] [18].

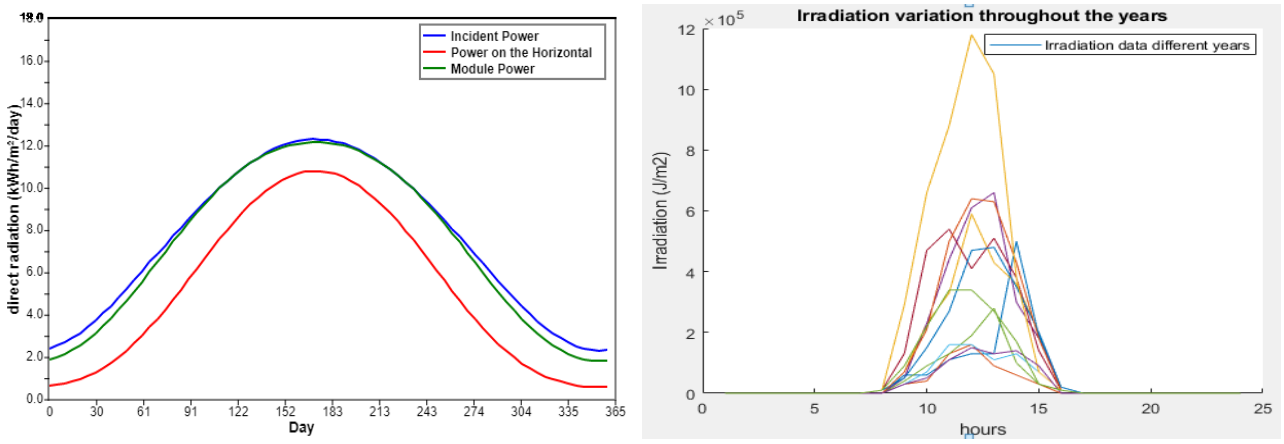

Figure 4: Approximation of how much optimal tilt angle compares to a horizontal panel [19]. Irradiation data used for every year of the project, every year uses data from a different year.

The KNMI irradiation data is given as the global horizontal irradiation (GHI) in J/m^2 [20] [21]. The data are on an hourly timescale, each hour indicated with subscript *h* in the equations given below. Because the PV panels are assumed to be tilted at a certain angle (optimal angle in this location being 37° [22]), the irradiance which effectively hits the panel is different from the GHI. To calculate the irradiation on the panel, the following approach is taken: The left side graph gives different radiation values for the optimal tilt angle at a certain latitude. The graphs for power on the horizontal and module power at optimal tilt angle are fitted with equations. Using the difference between these equations the effect of the optimal tilt angle is approximated for every day of the year considered in the model. All hours of a certain day use the same factor.

The temperature of the solar cells has impact on the efficiency of the solar panels. Solar cell temperature is calculated by the following equation [14] [18]:

$$T_h^c = T_h^a + \left(\frac{0.32}{8.91 + 2v_h}\right) G_h \quad (1)$$

With T_h^c being the cell temperature, T_h^a being the ambient temperature given in °C [20], v_h being the windspeed in m/s [20] and G_h being the solar irradiance on the panel. The efficiency of the solar panel is calculated next using [14] [18]:

$$\eta_h^{PV} = \eta^{ref}[1 - \beta^{ref}(T_h^c - T^{ref})] \quad (2)$$

With η_h^{PV} being the PV efficiency, η^{ref} being the efficiency at standard test conditions (value used here is 0.165 [23]), β^{ref} being the temperature coefficient of the solar panel (-0.42%/°C being the value used [24] [25] [26] [27]) and T^{ref} being the temperature at standard test conditions. Power production is finally calculated by the following equation [14] [18] [28]:

$$P_h^{PV} = A^{PV} G_h \eta_h^{PV} \tau^{PV} \quad (3)$$

With P_h^{PV} being the PV power production and τ^{PV} being a loss factor that takes into account module surface soiling and power conversion losses (0.846 is the value used [29]), A^{PV} being the total PV area. The PV area is one of the decision variables used and optimally determined in the model.

2.3 Wind energy

Weather data for Hoogeveen is also taken from KNMI [20], and this is then fed into a wind power production algorithm to calculate power production. Figure 5 shows the wind data being used over one week for all the different years. The variability is immediately apparent. The algorithm is based on methods and equations from [14] [14] [28]:

The average windspeed data for the hour at the measured height is transformed to the wind speed at hub height using the power law [14]:

$$v_h = v_h^i \left(\frac{Z}{Z_i}\right)^{\alpha} \tag{4}$$

The index *i* measured/reference condition. With v_h^i being the windspeed at the measured height in m/s, Z_i being the reference height (10 m is used [21]), *Z* being the wind turbine (WT) hub height (40 m [30]) and α being the power law coefficient (0.19 [31]), which is dependent on the type of land. The calculated windspeed at hub height is input for the power curve of the chosen wind turbine assuming standard air density (1.225 kg/m^3). This gives the power production of the wind turbine at standard air density. The power curve of the wind turbine is given by [14]:

$$P_h^{WT} =. \begin{cases} 0 & v_h \le v_{cut-in} \text{ or } v_h \ge v_{cut-out} \\ P^r \dfrac{(v_h - v_{cut-in})}{(v^r - v_{cut-in})} & v_{cut-in} \le v_h \le v^r \\ P^r & v^r \le v_h \le v_{cut-out} \end{cases} \tag{5}$$

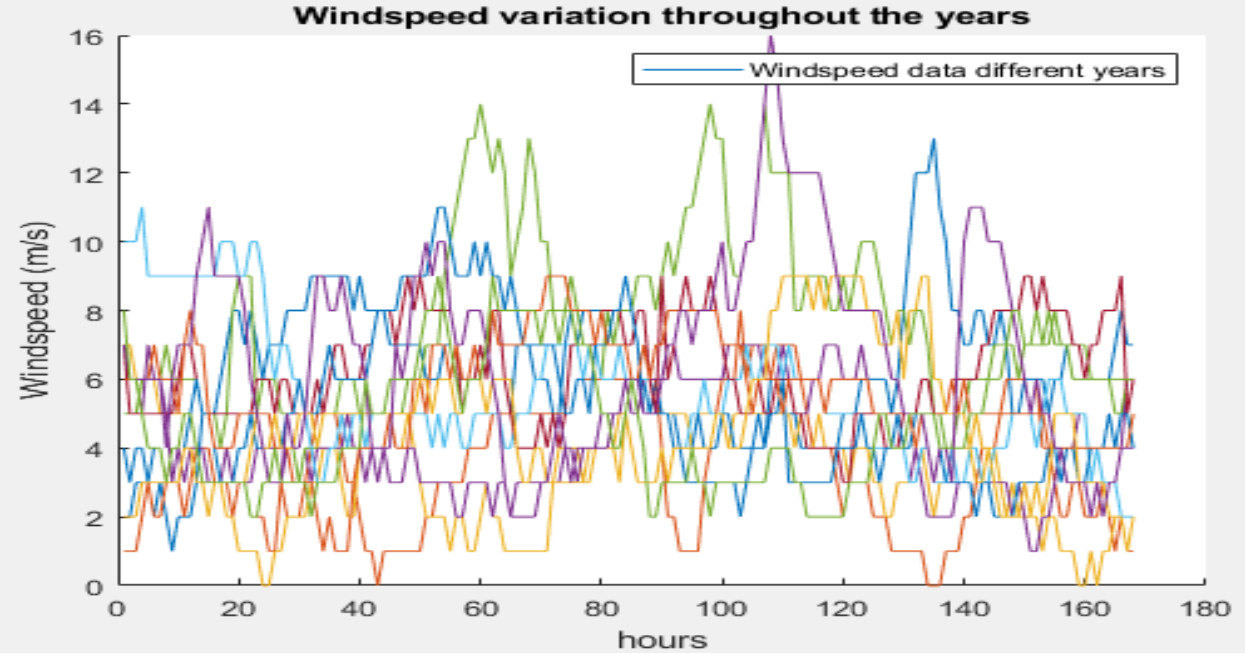

Figure 5: Windspeed variation of the data used.

With the cut-in windspeed being 2.5 m/s, cut-out windspeed being 20 m/s, rated windspeed being 7.5 m/s and the rated power of a turbine being 60 kW [30]. Between cut-in and rated windspeed, the power curve is fitted with a polynomial to get accurate numbers. Finally the power production by wind power is calculated by multiplying the wind turbine production by the number of turbines *N* and a loss factor τ^{WT} (0.88 is used [32]) which accounts for system downtime, misalignments, power conversions and wake effects [28]:

$$P_h^{wt,total} = P_h^{wt} N \tau^{WT} \quad (6)$$

The model optimizes for the amount of wind technology that needs to be installed to meet the demand at the lowest cost. Wind turbine capacity/number of wind turbines is one of the decision variables used and optimally determined by the model.

2.4 Grid electricity

Grid electricity is not modelled in detail and the approach is taken that the system can use grid energy when it cannot use other energy sources or if using grid electricity lowers the total cost. This assumption seems appropriate as it considers the grids greatest advantage, which is its immediate dispatchability characteristic. This also requires no complex modelling.

Capping grid electricity to create scenarios

Different constraints can also be used on grid electricity uptake in the model to approximate different scenarios. If no constraint is put on grid electricity use, it can represent no emission caps being put in place. A constraint on using no grid energy can represent the system being autonomous or major emission caps being put in place assuming grid electricity having high GHG emissions. Different number of caps on grid electricity can represent different scenarios of different emission regulations being put in place.

Grid electricity rate

In the Netherlands most providers offer either a fixed rate or a double rate. A few providers also provide spot market prices, but this would add too much complexity to this component. The fixed rate implies the price for grid electricity is always the same while the double rate charges a lower rate in off peak hours and a higher rate in peak hours. For Hoogeveen, the peak hours are from 7:00 to 23:00 and the off-peak hours from 23:00 to 7:00 [33] as per Rendo, which is the distribution system operator in Hoogeveen. The prices used in the modelling are based on [34] [35] (0.1965 EUR/kWh off peak and 0.2347 EUR/kWh for peak). Due to the most recent reference having comparable prices to the older one, it is assumed the price has not changed much and that the older rates are still applicable.

Setting the emission constraint

In order to set the grid constraints related to emissions, grid emission data and the targets for emissions reductions are used. For renewable energy supply chain projects in the EU, a minimum 70% emission saving compared to its fossil fuel reference is required from 2021 onwards and 80% from 2026 onwards [36] [37]. In this work only the electricity energy vector is used to set the emission constraint. The production of hydrogen via electrolysis must thus meet the emission reductions. The fossil fuel reference used is fossil generated electricity and its emission is taken to be 540 $grams_{CO2eq}/kWh_e$ as per [36] [38] [39]. For the onshore wind and PV technology the following values are taken for their emissions: 34.2 $grams_{CO2eq}/kWh_e$ for onshore wind and 91.1 $grams_{CO2eq}/kWh_e$ for crystalline silicon cells [40]. A 70% reduction means that the average kWh_e in the energy system for producing hydrogen can have a maximum emission of 162 $grams_{CO2eq}/kWh_e$ and for 80% this becomes 108 $grams_{CO2eq}/kWh_e$. The mathematical form of the emission constraint is given in the following chapter. The amount of grid energy bought is a decision variable and optimally determined by the model. The grid efficiency is taken to be 0.9, thus 10% losses due to all combined factors [41].

2.5 Battery system

The battery system is added to the energy system due to the intermittent nature of wind and solar energy generation. It has two purposes in the energy system being considered:

1. To act as an energy storage system thus, storing electrical energy when there is a surplus to use it later when there is a deficit. This can be to meet the electricity demand or as electrical energy input to the electrolyser to produce hydrogen to meet the heating and/or mobility demand.
2. To smoothen the electrolyser operation which can be very dynamic/unsteady due to the intermittent renewable generation. The battery system can dampen this fluctuating operation and only operate in certain ranges of the nominal electrolyser output.

Choice of battery technology

Battery technology was chosen based on the following characteristics: lifetime of the battery system compared to the energy system as a whole, short-term storage (seconds-minutes range) for steady electrolyser operation, long-term storage (daily weekly range) to cover intermittent renewable generation gaps and finally low costs which is always considered. the battery system that most meets the criteria and thus chosen is a vanadium flow battery. This choice is backed up by characteristics mentioned for redox flow batteries in general such as high voltage, good reversibility, the use of low cost and abundant active materials, high energy density, stability in aqueous solution, long life cycle, high efficiency, capability of being fully discharged and design flexibility which translates to excellent scalability into large scale storage [42] [43].

Modelling the battery

Modelling of redox flow batteries can vary from more microscopic models such as the ones reviewed in [42] to more macroscopic experimental data driven models such as done in [44]. Due to lack of data and the burden of computational time neither of such approach was taken. This means that factors such as how quickly it can be charged or discharged and how much energy can be cycled through it before needing a replacement, which are included in the modelling of [14] are not implemented. However, due to the capacity of redox flow batteries being a function of the amount of active material stored and the active material being stored externally leading to no self-discharge, coupled with the power rating being a function of the battery chamber size, makes it possible to independently select these parameters for an application [43]. This coupled with full discharge capability makes simplifying the modelling more acceptable. Thus battery operation is modelled as a general energy storage model using the characteristics and parameters of the vanadium redox flow battery according to the similar approaches employed by [11] [14] [45] [46]. Charge and discharge efficiencies are assumed to be equal at 0.866 giving a battery round-trip efficiency of 0.75 [47] [48] [49].

2.6 Electrolyser

The system consists of an electrolyser to produce the hydrogen to meet heating and mobility demand. Electrolyser technology is chosen based on the following characteristics: technological maturity, capability to be coupled to renewables such as solar and wind, fast response time to respond to intermittent fluctuations and the lifetime of the electrolyser. The electrolyser technology that most meets the criteria and thus chosen is Proton Exchange Membrane (PEM) electrolysis. The choice of using PEM electrolysers over alkaline electrolysers, which are the two on the market technologies is backed up by the following characteristics: the higher current densities which are achievable and the use of polymer membranes that make the gas qualities and partial load tolerance of PEM electrolysers better suited to intermittent operation and strongly differentiating inputs than alkaline electrolysers [50]. The electrolyser operation is modelled as done in [7] [28] [51]:

$$HP_{EL,h} = \frac{\eta^{EL} P_h^{EL}}{HHV_{H2}} \quad (7)$$

With $HP_{EL,h}$ being the amount of hydrogen produced in kg at hour h, η^{EL} being electrolyser system efficiency, P_h^{EL} being the power used by the electrolyser in kW and HHV_{H2} being the higher heating value of hydrogen in kWh/kg.

Aspects not included in electrolyser modelling

This is a simplified modelling approach, which does not take into account the changing electrolyser system efficiencies under different loads. The load affects almost all operation parameters such as electrolyser current densities, pressure level and temperature, which in turn influence the system efficiency [52]. With a detailed model which incorporates all these interconnected relationships lacking, an approach to include the changing system efficiency is using experimental data of efficiency and partial load of the considered technology. Non-linear data can be linearized in this case with an incremental linearization technique such as done in [53]. However, this gives added complexity and computational time for slight improvements and is thus not pursued.

Data used for electrolyser

Data from the PEM electrolyser system from Siemens for the Energiepark Mainz project is used to get an indication of the operating performance of current state of the art PEM systems. This is shown in Figure 6 [54].

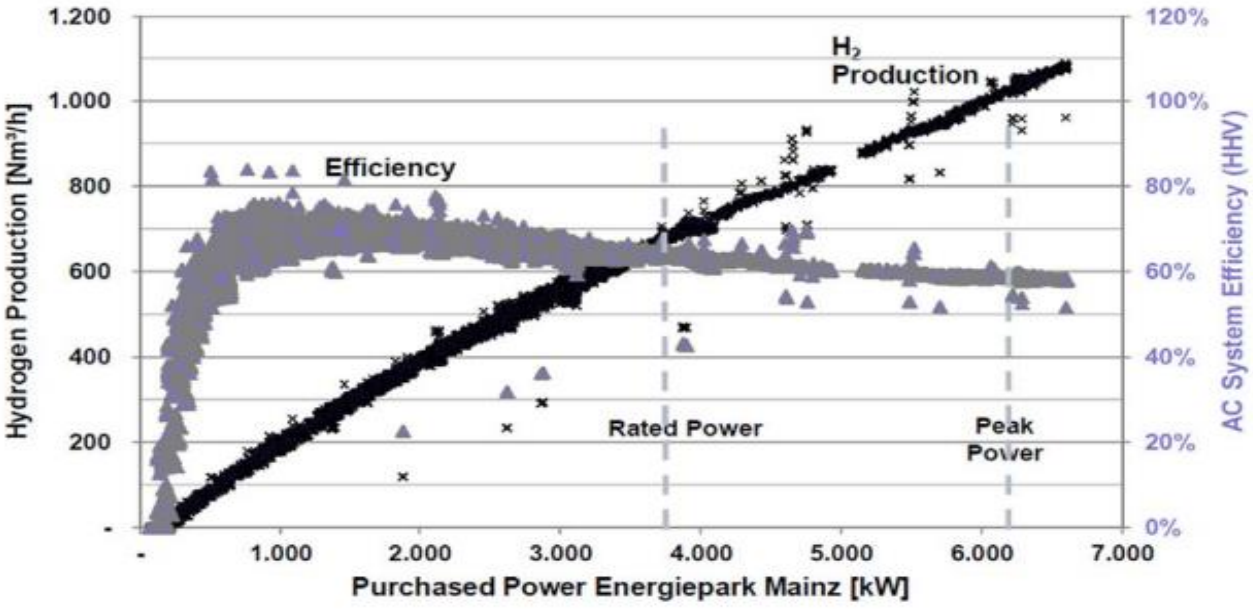

Figure 6: Efficiency of the PEM system of Energiepark Mainz as a function of power consumption [54].

It can be seen that the system efficiency increases from peak power (165% of rated power, η_{LHV} = 49%) through rated power (3.75 MW, η_{LHV} = 55%) till a certain % of part load operation (27% rated power, η_{LHV} = 64%) after which there is a declining pattern. The efficiencies are system efficiency not stack efficiency and include Balance-of-Plant (BoP) (cooling, purification and compression to 80 up till 225 bar). Up until 18% rated power, the efficiency is still comparable to rated power, the average over this range being an estimated 58% and this value is used in the calculations.

Electrolyser system assumptions

The electrolyser is also assumed to be able to have very fast response times, that can handle the fluctuating intermittent generation. This seems to be a reasonable assumption seeing the time scale of the model being one-hour intervals, while response times of about 0.2 s have been reported for PEM electrolysers [55]. Typical pressures for PEM electrolysers are between 20-50 bar, although very high pressures of around 345-448 bar

for direct filling of hydrogen vehicles has been demonstrated for PEM electrolysis [54]. The system efficiency used, which is from the Mainz project considers pressures of 80 up to 225 bar. For the Hoogeveen project, the heating demand storage pressure is projected to be at 80 bar [16]. It can be thus assumed that the electrolyser being used can deliver the hydrogen at the pressure required for heating demand storage. This takes away any other compression costs related to heating demand storage. Electrolyser output pressure is taken to be 100 bar, which leaves some room for pressure loss during transportation to the heating demand storage.

2.7 Hydrogen storages, heating network and refueling for mobility components

Gaseous hydrogen storage is chosen as the most apt technology. This is chosen over liquified and cryo-compressed storage. This is because cryo-compressed storage is still in the research and development stage and liquified hydrogen storage is used for medium to large scale storage and transportation of hydrogen over large distances (truck delivery and intercontinental hydrogen shipping) to locations with high demands [56]. The heating storage pressure needs to be 80 bar [16], but this is within the possible output pressures of the electrolyser. This means there is no compression and thus no need to include possible compression costs for the heating demand storage.

Volumetric storage size calculation

The hydrogen flows are tracked in kWh, but the storage size is also given volumetrically to get a spatial indication of its size. It is assumed that the hydrogen for heating is stored at 80 bar and around 10 °C, as the gas receiving station has to receive the hydrogen at a temperature between 5-20 °C [16]. For mobility this is 950 bar and around 10 °C. The real gas law can then be used with the assumed storage conditions and amount of hydrogen to calculate the volume needed for storage. The same approach is used to volumetrically size the mobility storage. The real gas law is given by [57]:

$$V_{storage,h} = \frac{m_{H2,,storage,h} Z_{H2} R_{H2} T_{storage}}{p_{storage}} \quad (8)$$

With $V_{storage,h}$ being the storage volume in m^3,$m_{H2,storage,h}$ being the amount of hydrogen in the storage tank in kg, *Z* being the compressibility factor of hydrogen at the considered conditions (1.65 for mobility and 1.04 for heating [58]), R_i being the specific gas constant in J/kg*K, *T* being the temperature inside the storage tank in K and *p* being the pressure inside the storage tank in Pa.

Heating network fixed cost components

The other component considered of the heating supply chain is the gas receiving station and network, which will be installed as given by [16]. To incorporate the cost of the gas receiving station and the pipeline network, the network costs given in [16] for 427 houses is assumed to scale linearly and is taken to be 875,000/427*80 = appr. 164,000 €. This is not a variable but will be included in the costs to give a more accurate indication.

Hydrogen refueling station protocol and fixed cost components

For the mobility side of the supply chain, the refueling infrastructure is needed to be able to deliver the dispensing service. The hydrogen refueling station (HRS) must comply with the fueling protocol, which dictates the process a station follows to safely fuel a compressed hydrogen storage system [59]. The EU uses the EN 17127 protocol, which references the more general J2601 protocol used in countries worldwide [59]. It sets the operational boundaries for different conditions such as temperature, pressure, fueling speed etc., which in turn fixes the type of components/equipment a HRS needs. Figure 7

gives different design concepts that could be considered for a gaseous hydrogen supply. The optimization to find the minimized cost configuration can be an individual study on itself, but to simplify the case, the configuration needing the least amount of components is chosen. This is highlighted yellow in Figure 7 [60]. It can also be seen that no matter which configuration is chosen, there is a certain minimum amount/size of components that must be included. These are the heat exchanger, chiller and dispenser. The amount/size of these components depends on the station refueling capacity. [61] gives the performance specification of different size of HRS. The specification shows that a station with a maximum hydrogen throughput of 212 kg per day needs only one dispenser. [17] also studied different HRS configurations and concluded that up to a 300 kg/day throughput, one dispenser is enough. For this case which has a lower throughput these component sizes are thus fixed. For the configuration chosen, the other components needed are the high-pressure storage at 950 bar and the high-pressure compressor (must compress up to 950 bar) since the electrolyser is already included. The optimization thus determines the sizes of the storage needed, while the compressor costs need to be chosen based on the demand due to the non-linear nature of the compressor cost with size. The other fixed components costs are also given to give more accurate cost indications. The hydrogen storage modelling considers the mass balance of the tank. The mathematical representation will be given in the next chapter.

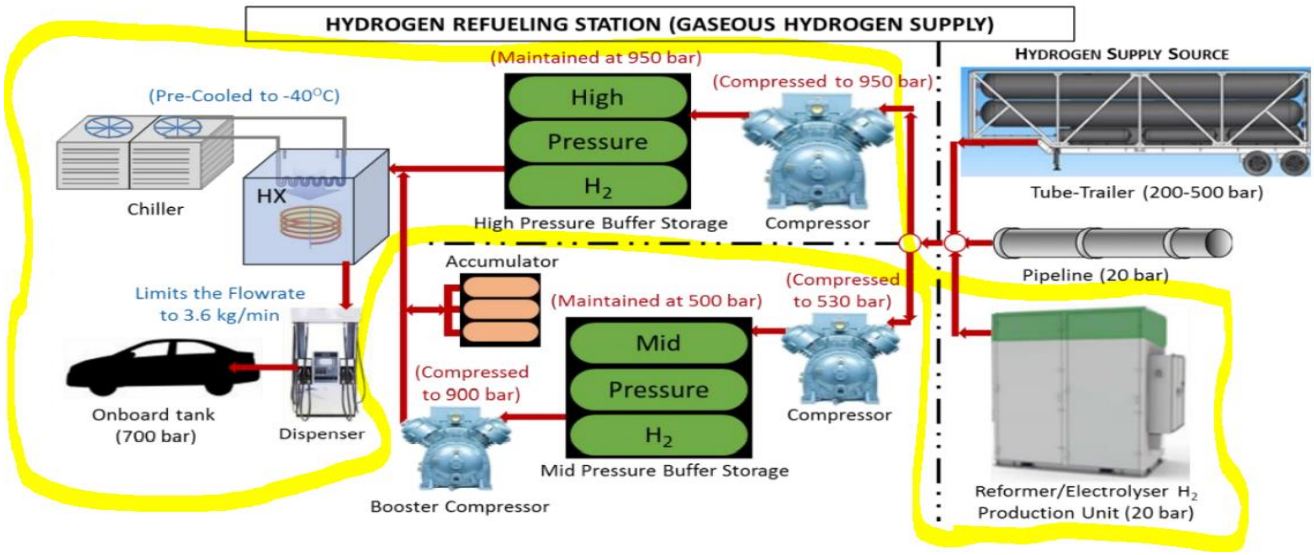

Figure 7: Possible refuelling station configurations for gaseous hydrogen [60].

2.8 Electricity demand profile generation

The electricity demand profile is obtained by using a model developed at EnTranCe [62]. The model simulates electricity loads at medium to low voltage transformers in residential areas. The transformers are connected to several households from which the loads are obtained. The households are modelled as objects where multiple characteristics of the object can be changed to generate different load profiles. Characteristics considered are the base load pattern, domestic PV pattern, heat pump pattern, EV pattern, battery system, demand side management system. These domestic characteristics are combined to produce the house net load. For this project, the houses are assumed to have only the base load characteristics. The load patterns are generated semi-randomly based on measurements. The base load pattern for this model is derived from Liander (one of the distribution system operators in the Netherlands) measurements of 80 houses for one year at 15-minute time intervals. The model runs for up to a 1-year period, with a timescale of 10 minutes for the given input. The model developed uses an hourly timescale, thus the

load pattern produced must be transformed from 10-minute intervals to hourly intervals. In order to incorporate the net zero house concept into this electricity demand pattern, the total electricity demand of a house is set to 3150 kWh, which is the amount of renewable energy generation/consumption needed to get the net zero energy certification [63]. The total consumption of the demand pattern generated by the model is divided by 3150, and the factor obtained is multiplied by all hourly intervals to get the required consumption, while maintaining the pattern.

2.9 Hydrogen heating demand profile

For the heating demand profile, the same demand profile is used as in the work by Hogewerf [15]. This is an hourly profile of heating demand for a year provided by N-tra, which is a subsidiary of Rendo, the regional distribution system operator for electricity, gas and heat. This heat demand profile is based on measurements of comparable houses to this project for the year 2017.

2.10 Hydrogen mobility demand profile

In order to produce a realistic synthetic hydrogen demand profile, the following approach and data is used from around 400 Chevron gasoline fueling stations [10,64,65]. Because hydrogen is also a fuel, the demand of gasoline is expected to translate well into hydrogen demand. The synthetic demand profile is obtained by: The average annual mileage of a personal vehicle in the Netherlands is given as 13,000 km/year [64]. The considered project consists of 80 houses and it is assumed that each house has a hydrogen powered vehicle. The fuel economy of the Toyota Mirai, which is one of the most popular hydrogen powered vehicles is used and is given as 106.2 km/kg H_2 [65]. The total amount of hydrogen needed for one year is thus 80*13,000/106.2= 9793 kg of hydrogen. This total yearly demand is mapped unto the weekly and daily distributions of fueling events provided by [66]. There is also a seasonal fluctuation which is taken into account. The demand is 10% higher in the summer period which is the 13 weeks from June to September and a corresponding decline in demand during the winter period from December to March [66]. After these steps a synthetic hourly demand profile for hydrogen mobility is obtained. The same profile is used for every year due to no demand evolution. To get the demand in kWh, the profile in kg must be multiplied by the HHV.

2.11 Optimizations performed

The model is used to find the lowest NPC and technological configuration for the whole system, for 21 scenarios. The scenarios analyzed are shown in Table 1. The following letters are used in the table: S - solar, W - wind, E - electricity, H - heating, M - mobility, B - battery and EC - emission constraint. E.g., SW-B-EC-M denotes an optimization where solar and wind is considered along with a battery system, emission constraint and mobility demand. These optimizations give insight into how the choice of solar or wind as a renewable energy technology influences cost and component deployment, how an emission constraint influences cost and component deployment and how a battery influences cost and component deployment for mobility and heating supply chains. The electricity optimization gives an indication what the cost would be compared to the grid price with some renewable component integration.

Unfortunately, no optimizations were performed with all demands present. This was due to time constraints and a lack of computational power. This will be elaborated on in the chapter 4.

Table 1: Different scenarios being considered by the optimisation model. The meaning of the letters is explained in the text. First column is heating, second is mobility and third is electricity optimisations.

S-H	S-M	-
S-EC-H	S-EC-M	-
W-H	W-M	-
W-EC-H	W-EC-M	-
SW-H	SW-M	-
SW-EC-H	SW-EC-M	-
S-B-H	S-B-M	S-B-E
S-B-EC-H	S-B-EC-M	-
W-B-H	W-B-M	W-B-E
W-B-EC-H	-	-

3 Mathematical Model

The model was programmed in MATLAB. This chapter gives the structured breakdown of the mathematical formulation of the model. The model needs to be structured in MATLAB around decision and slack variables, an objective function, equalities and inequalities, thus the structure of this chapter also follows this.

3.1 Decision variables, slack variables and non component cost parameter

Tables 2, 3 and 4 describe the decision variables, slack variables and parameters, respectively. In all tables, the subscript *h* means 'at hour h'.

Table 2: decision variables determined by the model with their description and unit.

Name	Description	Unit
x_1	Area of PV needed	m^2
x_2	Number of WT needed	Number of units
x_3	Battery capacity	kWh
x_4	Nominal electrolyser capacity	kW
x_5	Size of mobility hydrogen storage	kWh
x_6	Size of heating hydrogen storage	kWh
x_7	Total electricity bought from grid	kWh

Table 3: Slack variables with their description and unit at time h.

Name and unit	Description	Name and unit	Description
$E_{PV2ED,h}$ (kWh/h)	Flow of electricity from PV to electricity demand	$E_{batSOC,h}$ (kWh)	Amount of electricity in battery (state of charge)
$E_{PV2bat,h}$ (kWh/h)	Flow of electricity from PV to battery	$E_{EL,h}$ (kWh/h)	Total flow of electricity to the electrolyser
$E_{PV2EL,h}$ (kWh/h)	Flow of electricity from PV to electrolyser	$E_{H2,EL,h}$ (kWh/h)	Total amount of hydrogen produced
$E_{EL2HD,h}$ (kWh/h)	Flow of hydrogen from the electrolyser to hydrogen heating demand	$E_{EL2MS,h}$ (kWh/h)	Flow of hydrogen from the electrolyser to hydrogen storage for mobility
$E_{WT2ED,h}$ (kWh/h)	Flow of electricity from WT to electricity demand	$E_{EL2MD,h}$ (kWh/h)	Flow of hydrogen from the electrolyser to hydrogen mobility demand
$E_{WT2bat,h}$ (kWh/h)	Flow of electricity from WT to battery	HSM_h (kWh)	Amount of hydrogen in mobility storage (state of charge)
$E_{WT2EL,h}$ (kWh/h)	Flow of electricity from WT to electrolyser	$E_{EL2HS,h}$ (kWh/h)	Flow of hydrogen from the electrolyser to hydrogen storage for heating

$E_{grid2bat,h}$ (kWh/h)	Flow of grey electricity from grid to battery	HSH_h (kWh)	Amount of hydrogen in heating storage (state of charge)
$E_{grid2EL,h}$ (kWh/h)	Flow of grey electricity from grid to electrolyser	$E_{bat,ch,h}$ (kWh/h)	All electricity input flows for the battery (charging)
$E_{bat2EL,h}$ (kWh/h)	Flow of electricity from battery to electrolyser	$E_{bat2ED,h}$ (kWh/h)	Flow of electricity from battery to electricity demand
$E_{bat,dis,h}$ (kWh/h)	All electricity output flows from the battery (discharging)		

Table 4: Input data of the model with their description and unit at time h.

Name	Description	Unit
$P_{PV,h}$	PV electricity production per m^2 at time h	kWh/m^2
$P_{WT,h}$	WT electricity production per unit at time h	kWh/N
ED_h	Electricity demand at time h	kWh
HDH_h	Hydrogen demand for heating at time h	kg
HDM_h	Hydrogen demand for mobility at time h	kg
PGE_h	Price of grid energy at time h	€/kWh

3.2 Objective function

The main objective of the model is to minimize the levelized cost of the hydrogen produced by the system. The system considers three different products which are the electricity demand, hydrogen for mobility and heating. Because the levelized cost of energy (LCOE) equation is usually used for only one type of product in the supply chain, it was not sure how to combine all the products into this equation to get a proper comparison. Due to this it was decided to let the objective function be minimized in terms of the NPC of the system and after the optimization is done various LCOE figures can be calculated and related to each other to see how they compare. The problem is formulated as a linear programming (LP) problem on an hourly basis with 7 decision variables (see table 2), *n* being the expected lifetime of the system (in years, 12 years in this case), $y \in (1,2, \ldots, n)$ being a year in the lifetime of the system and $h \in (1,2,\ldots,8760*n)$ being a certain hour in the lifetime of the system. The objective function is given by:

$$NPC = \sum_{y=1}^{n} \frac{I_y + O\&M_y + E_y}{(1+r)^y} \quad (9)$$

where I_y is the investment costs in € in year y, given by:

$$I_y = \begin{cases} C_{1,CAPEX}.x_1 + C_{2,CAPEX}.x_2 + C_{3,CAPEX}.x_3 + C_{4,CAPEX}.x_4 + C_{5,CAPEX}.x_5 + C_{6,CAPEX}x_6 & y = 1 \\ C_{4,stack}.x_4, & y = 6 \; and \; 11 \end{cases} \quad (10)$$

CAPEX and OPEX cost parameters

CAPEX cost parameters are the following:

A PV module with an efficiency of 16.5% translates to roughly 165 Wp/m^2, this with a cost of around 850 €/kW_p = $C_{1,CAPEX} = 140$ €/m^2 [67] [68] [69] [70].

Using a cost of 1400 €/kW leads to a unit cost of $C_{2,CAPEX} = 84{,}000$ € per wind turbine [30] [70].

$C_{3,CAPEX} = 715$ €/kWh is used, this is the total system cost and includes BoP, power conversion system and construction and commissioning for the battery [71] [72] [73].
CAPEX for the electrolyser is taken to be $C_{4,CAPEX} = 1000$ €/kW based on several references [74] [75] [76].
For the electrolyser stack $C_{4,stack} = 320$ €/kW is used, stack lifetime is taken to be 45,000 hours so two replacements over the project financing period, the first is in the 6th year of the project and the second in the 11th year of the project [74]. The value of y_{stack} is thus 6 and 11.
CAPEX of the mobility high pressure storage is taken to be $C_{5,CAPEX} = 1900$ €/kg [77] [78] [79] and for the lower pressure heating storage $C_{6,CAPEX} = 700$ €/kg [77] [79].

O&M$_y$ is the operations and maintenance costs in € in year y, which is given by:

$$O\&M_y = C_{1,OPEX}.x_1 + C_{2,OPEX}.x_2 + C_{3,OPEX}.x_3 + C_{4,OPEX}.x_4 + C_{5,OPEX}.x_5 + C_{6,OPEX}.x_6 \quad (11)$$

OPEX cost parameters are the following:
For PV 17 €/(kW$_p$.a) is used from a combination of the various references, translates to $C_{1,OPEX} = 2.8$ €/(m^2.a) [67] [68] [69] [70].
The OPEX for wind turbines is taken to be 25 €/(kW.a). One unit is thus $C_{2,OPEX} = 1500$ €/(unit.a) [70] [80].
Battery OPEX is taken to be 2% of CAPEX per year. This translates to $C_{3,OPEX} = 14$ €/(kWh.a) [73].
Electrolyser OPEX is assumed to be 5% of CAPEX and is thus $C_{4,OPEX} = 50$ €/(kW.a) [74] [75].
For the mobility high pressure storage no specific reference was found with regards to OPEX. Thus 3% of CAPEX is used as an estimate compared to the 2% of the lower pressure storage due to higher pressures. This translates to $C_{5,OPEX} = 57$ €/(kg.a).
2% of CAPEX for the heating storage translates to $C_{6,OPEX} = 14$ €/(kg.a) [81].

E_y is the electricity costs in € in year y, which is given by (the cost per kWh used is given in the grid section and is equal to $C_{7,h}$):

$$E_y = \sum_{h=(y-1).8760+1}^{8760.y} C_{7,h}.x_{7,h} \quad (12)$$

And *r* is the discount rate (0.07 is the value used, assuming no inflation [82]).

Postprocessing and fixed costs
Following the computation of the optimized NPC, the following postprocessing is done: the NPC of fixed costs such as the heating network and HRS is added to this cost (this is $NPC_{fixed,heating+refueling}$) to get the total NPC. Obviously these costs are added only if the configuration optimised consists of the mobility or heating supply chain. The calculation of the fixed NPC is the same as the optimisation, only that the values are fixed. The heating network fixed CAPEX is taken to be **164,000** € [16]. For the refueling station fixed CAPEX, estimates without compressor and storage costs range from 500,000 € to 950,000 €. Compressor costs are estimated at 162,500 € for 50 kg/day 2.3 kg/h 10-12.5 kW, 208,000 € for 100 kg/day 6kg/h 25 kW, 359,000 € for 200 kg/day 14kg/h 60 kW, 494,000 € for 300 kg/day 23 kg/h 100 kW. The smallest compressor is taken and midrange of the further costs giving **887,500** € without storage [17] [83].
For fixed OPEX 4% of CAPEX is taken for the heating network, which translates to 6560 €/y [77].

5% of CAPEX is used for the refueling station OPEX, which translates to 44375 €/y [81]. For the refueling station compression and precooling costs, 0.4 kWh/kg H_2 for precooling and 1.6 kWh/kg H_2 for compression is used [77] [81]. The same price per kWh is used as $C_{7,h}$.
The general expression for the calculation of LCOE, whatever the end application is given below and is termed the levelized cost of combined electricity and hydrogen (LCOCEH) (€/kWh is the unit calculated):

$$LCOCEH = \frac{NPC + NPC_{fixed,heating+refueling}}{\sum_{y=1}^{n} \frac{ED_y + HDH_y + HDM_y}{(1+r)^y}} \quad (13)$$

This metric assumes a unit of energy over the whole system has the same value no matter what the end application is.

3.3 Constraints

Equalities

The following equalities were defined for defining the problem:

For each h, PV power production is equal to the PV power production vector multiplied by the decision variable, which is equal to all the power from PV to different components:

$$P_{PV,h}.x_1 = E_{PV2ED,h} + E_{PV2bat,h} + E_{PV2EL,h} \quad (14)$$

For each h, the same applies for the wind turbines but with the other vector:

$$P_{WT,h}.x_2 = E_{WT2ED,h} + E_{WT2bat,h} + E_{WT2EL,h} \quad (15)$$

For each h, the total grid power which is used is equal to all flows from the grid to the system:

$$x_{7,h} = E_{grid2bat,h} + E_{grid2EL,h} \quad (16)$$

For each h, the electricity demand vector gives the demand and this is equal to all power flows to the demand:

$$ED_h = E_{PV2ED,h} + E_{WT2ED,h} + E_{bat2ED,h} \quad (17)$$

For each h, the electrolyser power consumption is equal to all flows to the electrolyser:

$$E_{EL,h} = E_{PV2EL,h} + E_{WT2EL,h} + E_{grid2EL,h} + E_{bat2EL,h} \quad (18)$$

For each h, electrolyser hydrogen energy conversion is equal to power input multiplied by electrolyser efficiency.

$$E_{H2,EL,h} = \eta_{EL} E_{EL,h} \quad (19)$$

For each h, electrolyser hydrogen production is equal to hydrogen flow to the hydrogen for heating storage, hydrogen heating demand, the hydrogen for mobility storage and hydrogen mobility demand:

$$E_{H2,EL,h} = E_{EL2HS,h} + E_{EL2MS,h} + E_{EL2HD,h} + E_{EL2MD,h} \quad (20)$$

For each h, the amount of energy stored in the battery is equal to the energy in the battery the previous time step, plus all the power charged into the battery multiplied by the charging efficiency or minus the power out of the battery divided by the discharge efficiency:

$$E_{batSOC,h} = E_{batSOC,h-1} + \left(\eta_{ch} E_{bat,ch,h} - \frac{\left(E_{bat,dis,h}\right)}{\eta_{dis}}\right) \quad (21)$$

With:

$$E_{bat,ch,h} = E_{PV2bat,h} + E_{WT2bat,h} + E_{grid2bat,h} \; and \; E_{bat,dis,h} = E_{bat2EL,h} + E_{bat2ED,h} \quad (22)$$

For all storage, the storage level at the start is equal to the storage level at the end:

$$E_{batSOC,h=0} = E_{batSOC,h-(12*8760)} + \left(\eta_{ch} E_{bat,ch,h=0} - \frac{\left(E_{bat,dis,h=0}\right)}{\eta_{dis}}\right) \quad (23)$$

For each h, hydrogen storage level for mobility/heating is equal to hydrogen storage level of the previous time step plus hydrogen flow from the electrolyser to the specific storage, minus hydrogen flow to demand for mobility/heating:

$$HSM_h = HSM_{h-1} + E_{EL2MS,h} - E_{MS2D,h} \quad (24)$$

$$HSH_h = HSH_{h-1} + E_{EL2HS,h} - E_{HS2D,h} \quad (25)$$

Hydrogen demand is equal to the hydrogen from electrolyser to demand plus the hydrogen from storage to demand:

$$HDM_h = E_{MS2D,h} + E_{EL2MD,h} \quad (26)$$

$$HDH_h = H_{HS2D,h} + H_{EL2HD,h} \quad (27)$$

For all storage, the storage level at the start is equal to the storage level at the end:

$$HSM_{h=0} = HSM_{h-(12*8760)} + E_{EL2MS,h=0} - E_{MS2D,h=0} \quad (28)$$

$$HSH_{h=0} = HSH_{h-(12*8760)} + E_{EL2HS,h=0} - E_{HS2D,h=0} \quad (29)$$

Inequalities

The following inequalities were defined for defining the problem:

For each h, electricity stored in the battery must be equal to or less than storage capacity:

$$E_{bat,SOC,h} \leq x_3 \quad (30)$$

For each h, hydrogen stored in mobility or heating storage should be equal to or less than storage capacity:

$$HSM_h \leq x_5 \quad (31)$$

$$HSH_h \leq x_6 \quad (32)$$

For each h, power consumption of the electrolyser should be equal to or less than electrolyser capacity:

$$E_{EL,h} \leq x_4 \quad (33)$$

Over the lifetime of the system, the grams$_{CO2eq}$/kWh$_e$ (values of the coefficients given in the grid section of chapter 2) used in the system must be equal to or less than:

$$E_{WT2EL,h}\,34.2 + E_{WT2bat,h}34.2 + E_{WT2ED,h}34.2 + E_{PV2EL,h}\,91.1 + E_{PV2bat,h}91.1 + E_{PV2EL,h}91.1 + E_{grid2EL,h}540 + E_{grid2bat,h}540 \leq (1 - ER)540E_{demand,total,h} \quad (34)$$

With $E_{demand,total,h}$ being all the variables on the left side of this inequality and ER being the fraction representing the emission reduction %.

The total energy flow that can be charged into the battery is smaller than the battery capacity minus the state of charge of the previous timestep:

$$\eta_{ch}E_{bat,ch,h} \leq x_3 - E_{batSOC,h-1} \quad (35)$$

The total energy flow that can be discharged from the battery is smaller than the state of charge of the previous timestep. This is also the case for the hydrogen storages:

$$\frac{E_{bat,dis,h}}{\eta_{dis}} \leq E_{batSOC,h-1} \quad (36)$$

$$E_{MS2D,h} \leq HSM_{h-1} \quad (37)$$

$$E_{HS2D,h} \leq HSH_{h-1} \quad (38)$$

All decision and dummy variables are non-negative (E is the set containing all dummy variables):

$$x_i \geq 0\ with\ i = \{1 \dots 7\}\ and\ E \geq 0 \quad (39)$$

4 Results and discussion

The optimizations were performed using the MATLAB software on a remote desktop with an unknown CPU and 32 GB RAM memory. The linear programming algorithm that is used for the solver is the dual simplex algorithm. The following graphs are given of the wind, heating, battery with emission constraint scenario (W-B-EC-H) as to see how this system would need to perform to deliver the lowest cost system. This is done only for one out of the 21 scenarios as an example of how the optimization determines operational performance of the system. The confirmation of system operation being realistic for one scenario is deemed applicable to all other optimization due to using the same method. The most important variables are all plotted in Figure 8 and Figure 9 for a week in the winter (week 7) and in the summer (week 30) to see differences in operation. The operation of each other component of the system is also given over a year to see the general trend of how these certain components of the system perform over a year. The x-axis starts January 1 and ends on December 31.

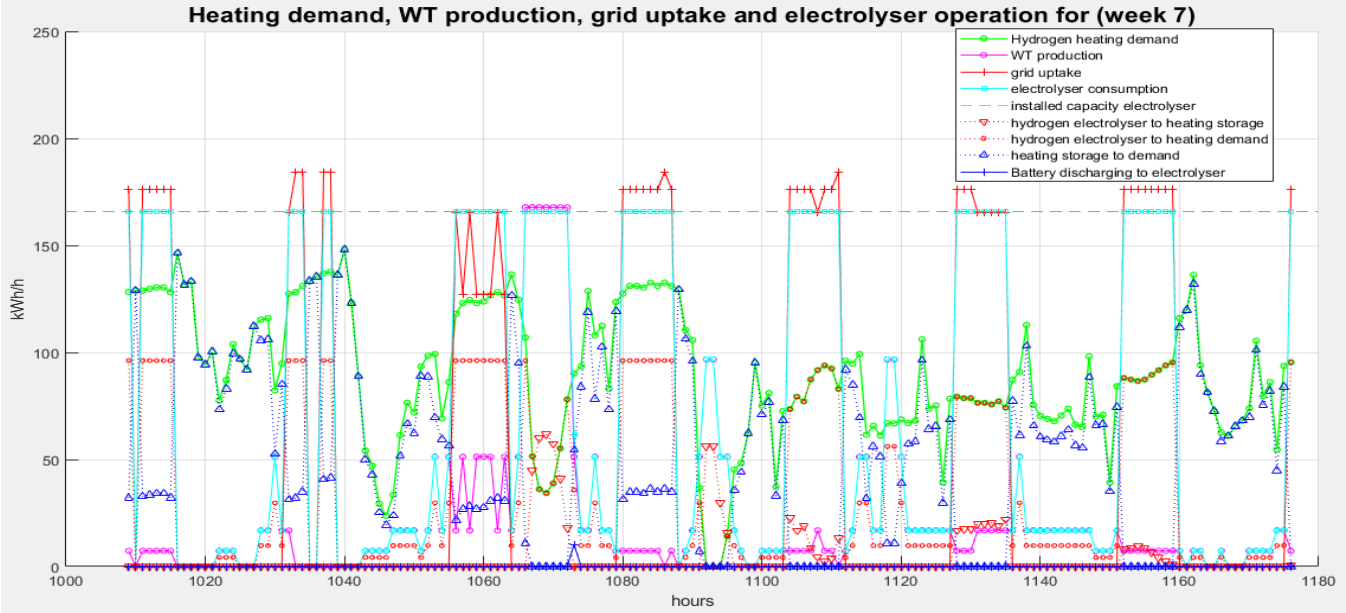

Figure 8: heating demand, WT production, grid uptake, electrolyser operation and heating storage flows for week 7 of a year.

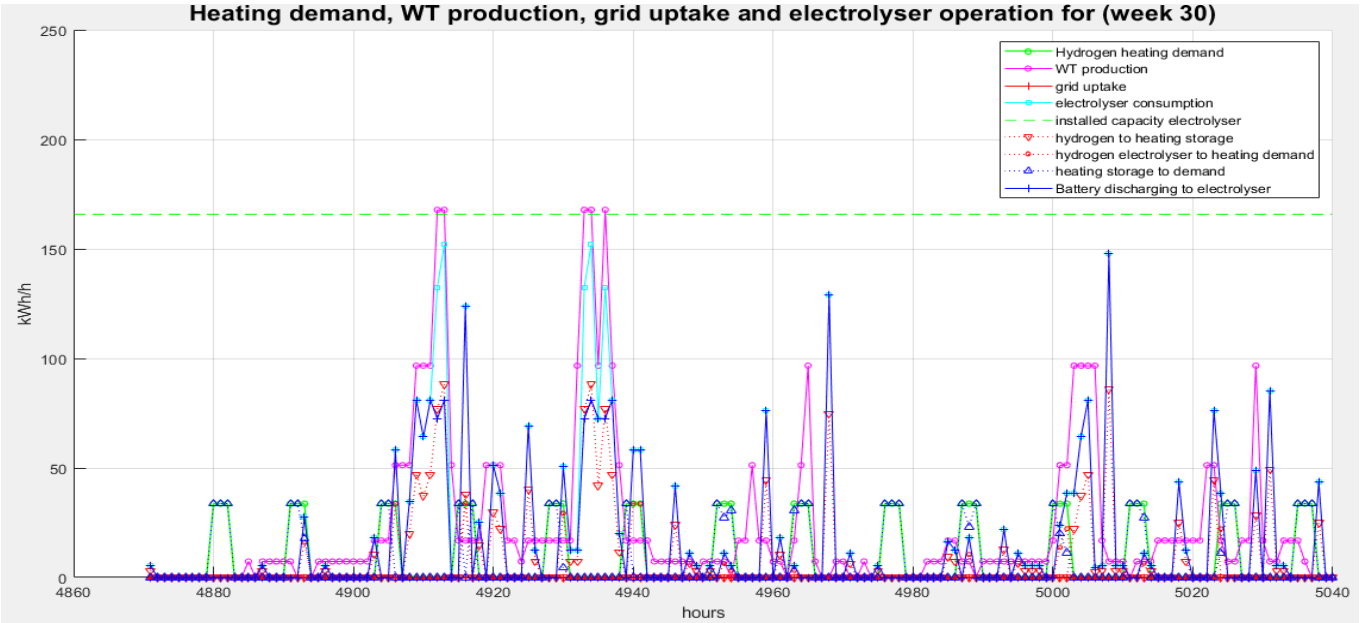

Figure 9: heating demand, WT production, grid uptake, electrolyser operation and heating storage flows for week 30 of a year.

Operational performance W-B-EC-H scenario

Figure 8 and Figure 9 give the contrast in operation between winter and summer operation for the optimized W-B-EC-H scenario. Some of the most notable differences are the much higher heating demand in the winter compared to the summer. This obviously has massive effects on the rest of the system operation due to it being demand driven. This explains the difference in operation. Notable is that only the winter week has grid uptake. The grid uptake is also at a high capacity compared to the electrolyser capacity and heating demand. WT production is less in this particular winter week than the summer week. One factor that could effect the models accuracy is the electrolyser consumption, which for the winter week uses rated capacity much more than the summer week, but both have many points at low partial load, which means the assumed system efficiency of the electrolyser does not hold up at these operating points. In practice, hydrogen production is expected to be less at these points. The more of these operating points for the electrolyser, the less realistic the results. The electrolyser system efficiency rapidly decreases at around 18% rated capacity (figure 7). With an electrolyser capacity of 165.9 kW, this means all points under 29.9 kW are prone to error. From Figure 8 and Figure 9, a fair percentage of points are below this number.

The winter week has no usage of the battery at all, while the summer has many operating points where only the battery is used to operate the electrolyser, with many of these points occurring again at lower partial loads. Thus more grid usage in the winter and more battery usage in the summer. This makes sense as more grid usage leads to less battery usage due to grid uptake being immediately available.

The hydrogen storage for heating is used in both weeks to meet a significant part of the heating demand, while in the winter there are many points where hydrogen straight from the electrolyser contributes significantly to demand. For this certain week in the summer it seems that only the heating storage is used to meet demand and no direct flow from the electrolyser. For both weeks there are points which show hydrogen flow to the storage, but the storage is used much less in the summer, due to lower heat demand. More hydrogen heating storage flows to demand make sense due to higher heating demand in the winter. More flows straight from the electrolyser to demand also lines up with the increased grid uptake.

The main conclusion from these plots is that the results of the model can be made more accurate by including changing electrolyser system efficiencies depending on the load or incorporating a constraint which limits electrolyser load to certain ranges. The graphs also seem to indicate realistic operation with no strange trends appearing.

Trends of system components over the year

Figure 10 shows the battery operation over a year. Notable is the usage of the battery, which is much less during the colder months compared to the warmer months. The grid is not used at all to charge the battery. The usage of the battery is probably higher during the summer because of the limited use of grid electricity available due to the emission constraint. The higher demands occurring during the winter causes the system to choose to use most of the grid electricity allowed before the emission constraint is violated during this time. This leaves less available for the summer. In order to deliver the demand it is forced to use the battery during the summer.

Figure 11 shows the hydrogen heating storage operation for a year. The scale of the storage is much greater than the hourly hydrogen flows which charge/discharge the storage. The trend for the state of charge (SOC) of the storage seems to be discharging occurring primarily during the colder months while charging occurs during the warmer months. Notably the storage is full at the start of operation. This is probably due to operation being started in the winter. The constraints indicate that the end level of the storage should be the same as the start level, thus all energy supplied is accounted for by the demand. A less complex scenario was tested with a constraint forcing the storage to start empty, and the result was insignificant in regards to price. It would probably lead to more computational effort and thus it was chosen to do the optimizations without the forced empty starting SOC.

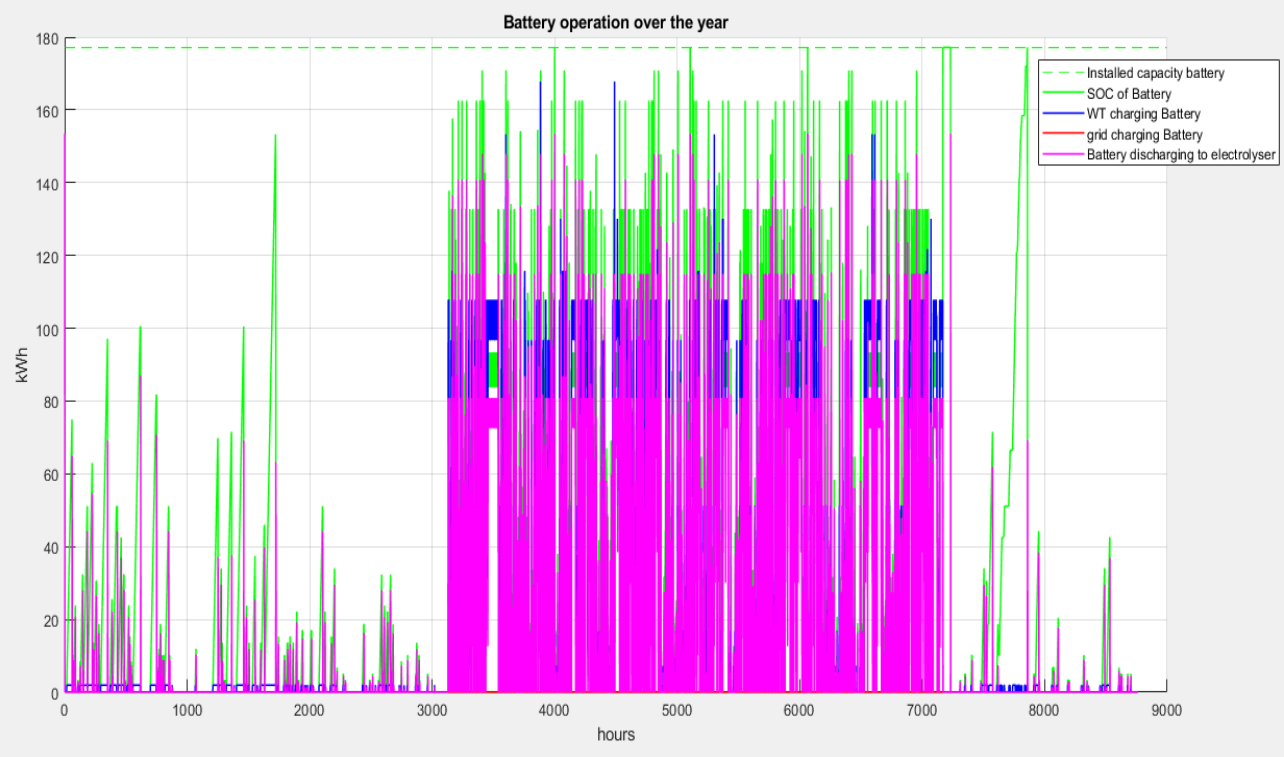

Figure 10: Battery operation over the first year of the project.

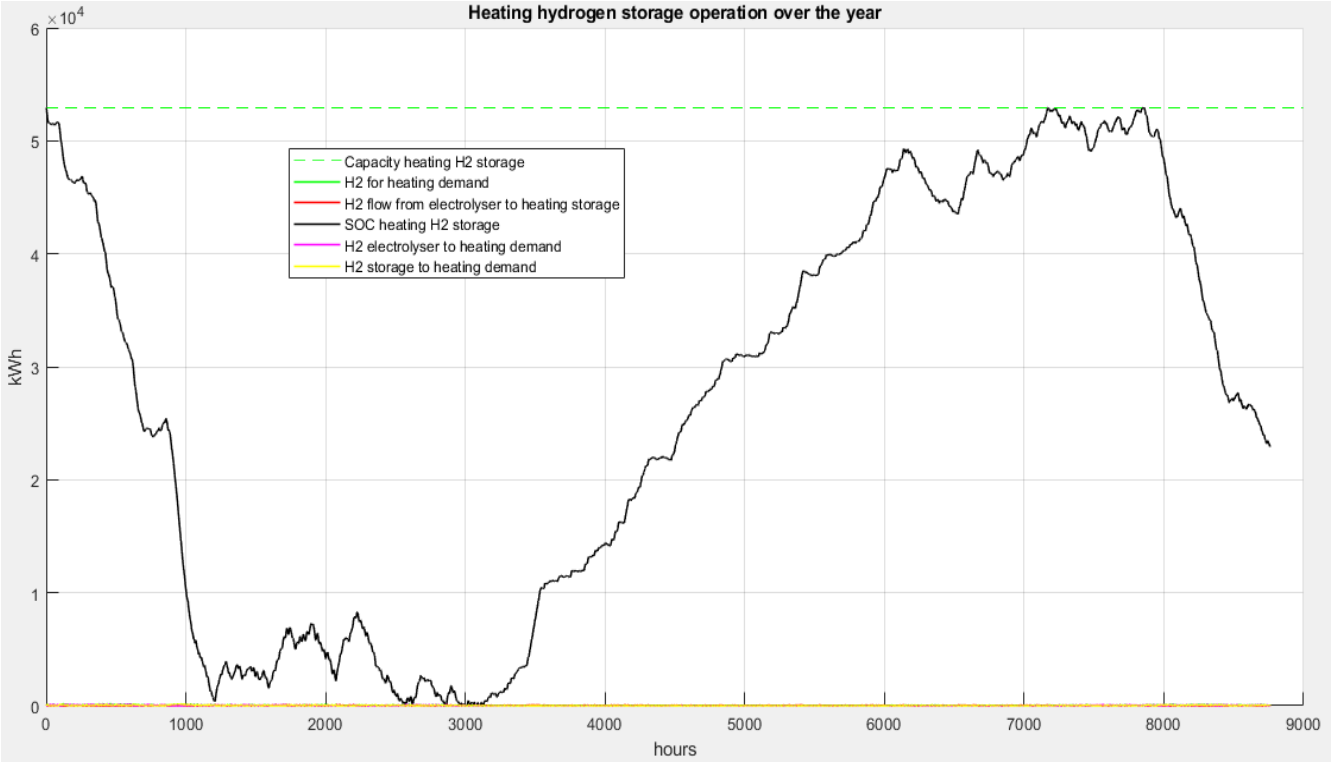

Figure 11: Heating hydrogen storage operation for a year.

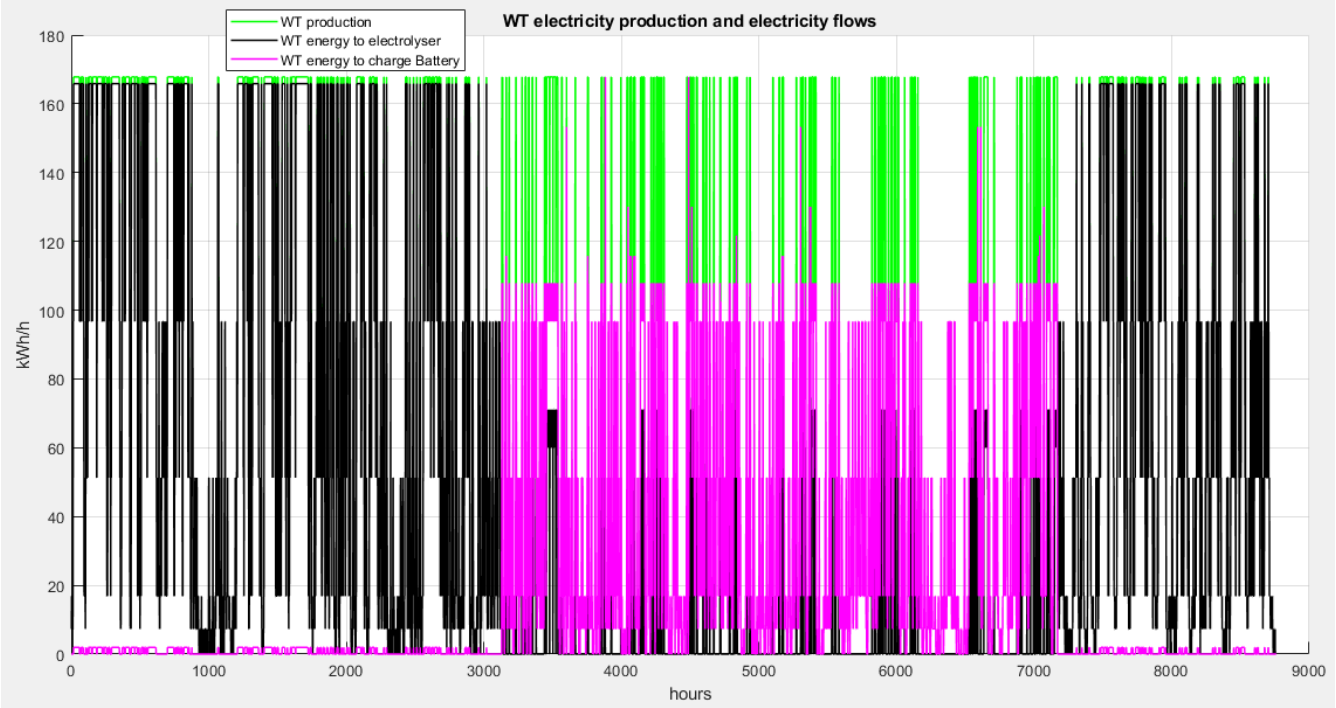

Figure 12: WT electricity production and electricity flows from the WT over a year.

Figure 12 shows the WT energy production and usage over a year. The trend of usage over this year seems to be directly using the energy to produce hydrogen during the colder months and a more balanced usage during the warmer months with most of the usage going to charging the battery. This trend fits the observation of the use of grid electricity during times of high demand and storage during warmer months mentioned earlier. There is less dispatchable generation available during the summer due to the emission constraint capping the grid energy and thus the battery is charged to guarantee operation. Figure 13 supports

the grid budget observation, with most of the grid uptake being in the colder months when there is higher demand. Using more grid uptake is probably not done in the summer months due to the emission constraint. It can also be seen that the grid is only used directly to the electrolyzer, thus no grid is used to charge the battery. So, the cost of grid energy is not low enough to cycle energy through the battery when the price is lower at non-peak time.

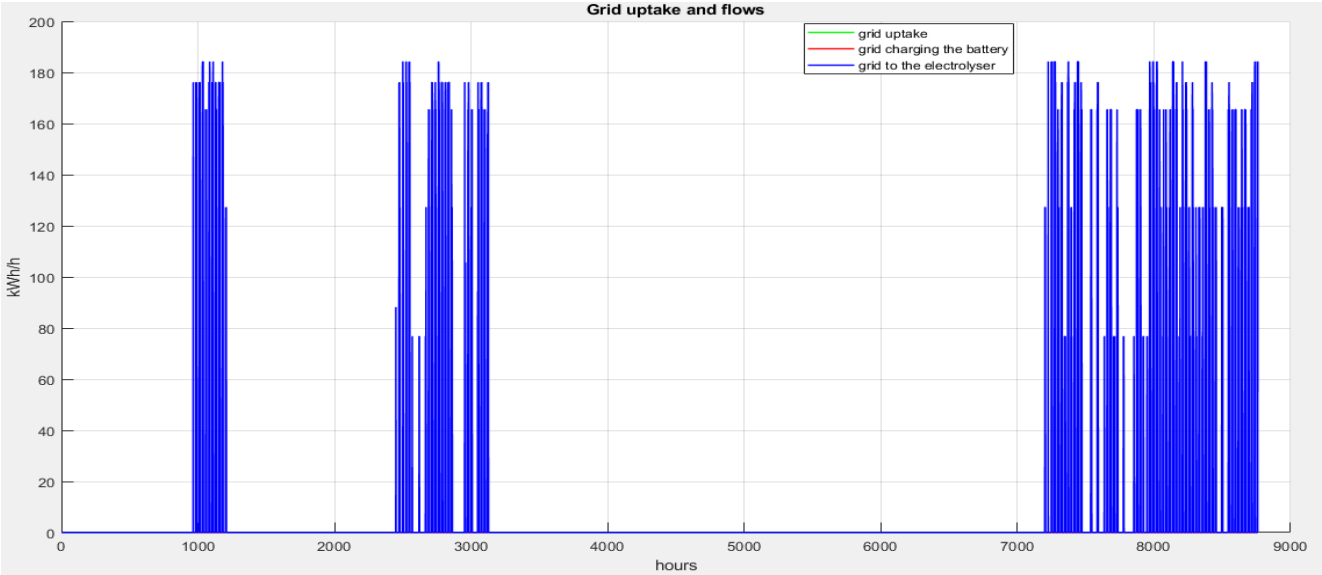

Figure 13: Grid uptake and flows over a year.

Figure 14 shows how the heating demand is met concurrently with the electrolyser operation over a year. Apparent is storage being used more with higher demands (colder months), hydrogen flow directly from the electrolyser to demand seems to be a consistent percentage of the demand throughout the year and the storage being charged more during times with lower demands (warmer months). The operational behaviour seems to be logically consistent throughout these graphs, with no strange trends apparent. The most important modelling observation being the possible error introduced due to the constant electrolyser efficiency assumption.

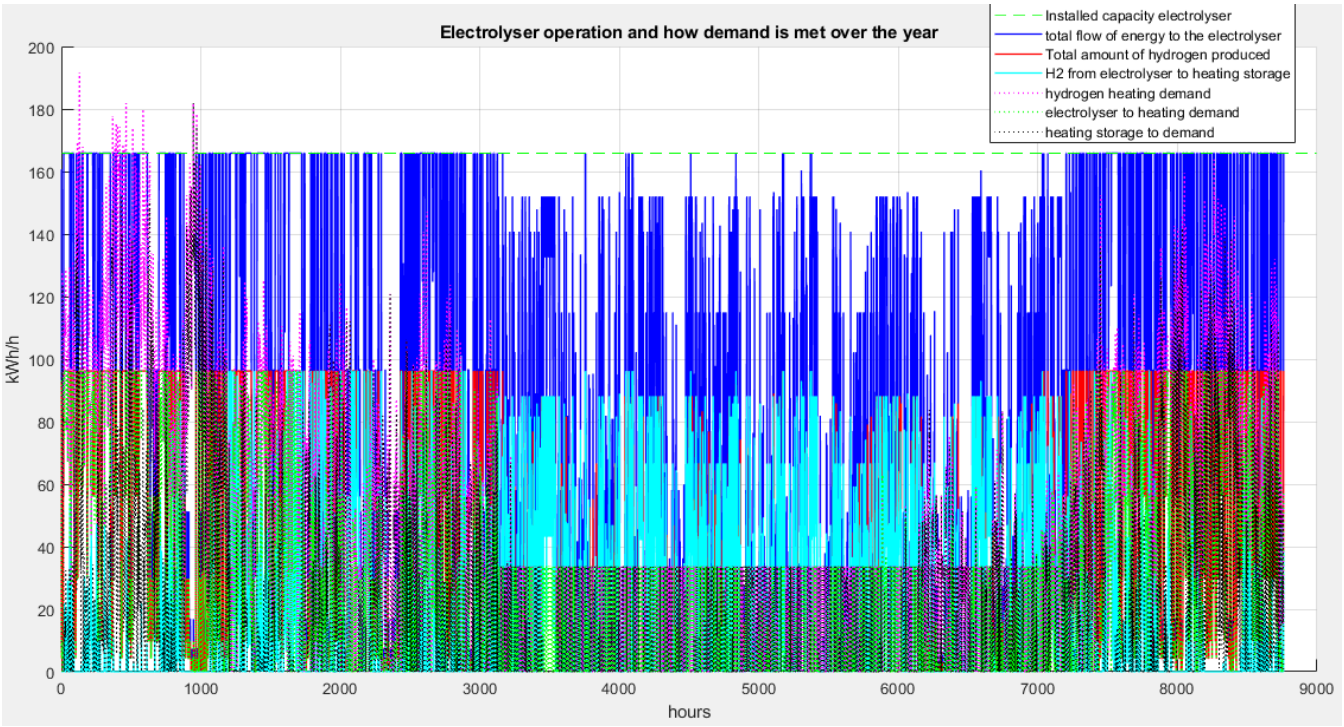

Figure 14: Electrolyser operation and how demand is met over a year.

Computational time aspect of optimization

Figures 15, 16 and 17 and table 5 give emissions, LCOH, component cost fraction and components sizes determined for the 21 scenarios. Unfortunately, it can be seen that the more complex configurations possible in the system design are not included. This is due to the computational time needed to perform these scenarios, hardware limits and time constraints which needed to be met. The more complex a scenario becomes the more variables must be determined by the optimization. Due to the 12-year project length and hourly resolution, every added variable that is not a fixed component value adds 105,120 extra variables to a scenario. To get an indication of the time needed, the least complex optimization scenario included in the tables has a solution time of around 1200 seconds on the used PC. The most complex optimizations performed, which are still some ways off the total system take upwards of one day. From this it can be deduced that with the available computational power, the more complex scenarios would take multiple days at the minimum to generate a solution. The time required to solve an optimization does not seem to scale linearly with the number of variables. This should be kept in mind for future work. The performed optimizations were separate configurations for the heating and mobility supply chain. A further two optimizations were performed for the electricity demand supply chain.

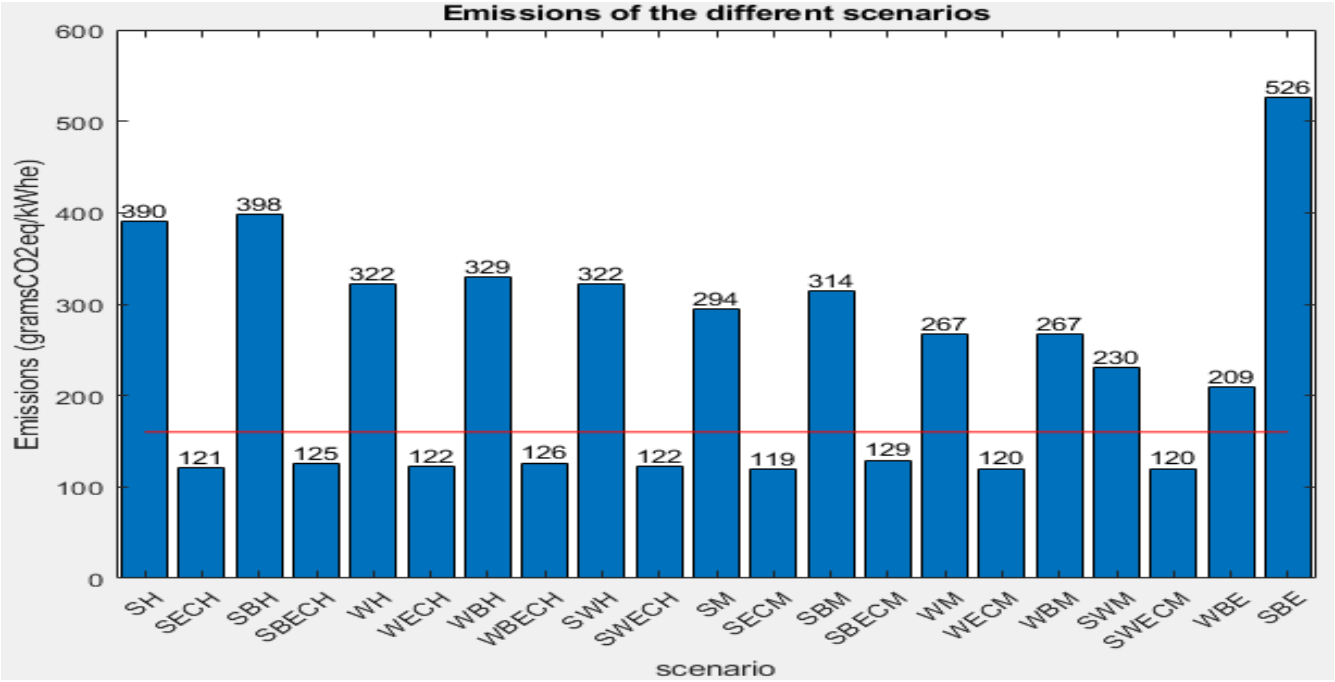

Figure 15: Emissions of the scenarios. (the orange line is the max allowed emission to comply with the constraint, 160 gramsCO2eq/kWhe).

Confirmation of emission constraint function

Figure 15 shows the emission for each scenario. It can be seen that all emission constraint scenarios comply with the constraint. Also there is still some emissions possible according to the graph. This is probably due to the intermittent nature of renewable generation. At peak generation when the resource is plentiful, the energy is cheaper than grid energy which leads to some deployment**.** This is up to a certain point. The emission constraint not being maxed out indicates that the point has not been reached where grid energy price is generally cheaper than the renewable deployment for these scenarios. The non emission constraint scenarios also indicate this due to all of them having a certain renewable deployment, when this is not forced.

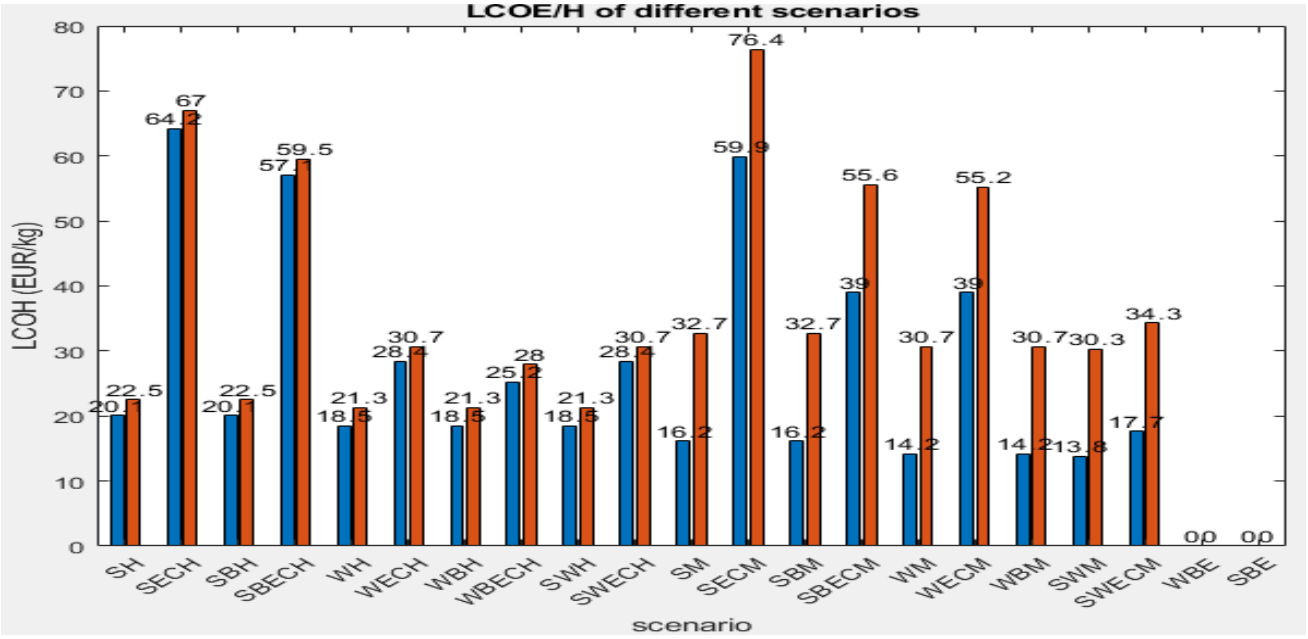

Figure 16: LCOH of the scenarios (blue is only variable costs and orange variable and fixed costs).

Table 5: Electricity generation and component sizing.

scenario	PV supply lifetime (MWh)	WT supply lifetime (MWh)	x1 (m^2)	x2 (real number)	x7 (MWh)	x3 (kWh)	x4 (kW)	x5 (kWh)/ (m^3)/ (kg)	x6 (kWh)/ (m^3)/ (kg)
S-H	920.8	-	364.2	-	8152.4	-	213.9	-	2193.4/ 8.45/ 55.7
S-EC-H	7065.3	-	2794.8	-	1325.2	-	442.5	-	197561/ 761.2/ 5014.2
S-B-H	920.8	-	364.2	-	8152.4	-	213.9	-	2193.4/ 8.45/ 55.7
S-B-EC-H	7316.4	-	2894.1	-	1372.3	352.94	351.3	-	159658/ 615.1/ 4052.2
W-H	-	2206.6	-	1.071	6723.8	-	182.8	-	7473.8/ 28.8 189.7
W-EC-H	-	6331.4	-	3.072	2140.6	-	162.2	-	74576/ 287.3/ 1892.8
W-B-H	-	2206.6	-	1.071	6723.8	-	182.8	-	7473.8/ 28.8/ 189.7
W-B-EC-H	-	6550.5	-	3.179	2214.7	177.15	165.9	-	52928/ 203.9/ 1343.4
SW-H	-	2206.6	-	1.071	6723.8	-	182.8	-	7473.8/ 28.8/ 189.7
SW-EC-H	-	6331.4	-	3.072	2140.6	-	162.2	-	74576/ 287.3/ 1892.8
S-M	2576.1	-	1019	-	5963	-	161.4	650/ 0.335/ 16.5	-
S-EC-M	6795.6	-	2688	-	1274.6	-	425.6	58979/ 30.4/ 1496.9	-
S-B-M	2590.5	-	1024.7	-	5947.3	0.877	161.2	649.5/ 0.334/ 16.5	-

S-B-EC-M	7330.3	-	2899.6	-	1374.9	705	302.9	23694.5/ 12.2/ 601.4	-
W-M	-	3058.2	-	1.484	5427.3	-	82.7	946.1/ 0.49/ 24	-
W-EC-M	-	6089.8	-	2.955	2058.9	-	156	39135/ 20.2/ 993	-
W-B-M	-	3058.2	-	1.484	5427.3	-	82.7	946.1/ 0.487/ 24	-
SW-M	914	2823.8	361.6	1.370	4672	-	127.7	1007.7/ 0.519/ 25.8	-
SW-EC-M	2723	3649	1077	1.771	1744.7	-	258.3	6930.9/ 3.57/ 175.9	-
W-B-E	-	2471	-	1.199	1011	194.3	-	-	-
S-B-E	861	-	340.6	-	2798	194.3	-	-	-

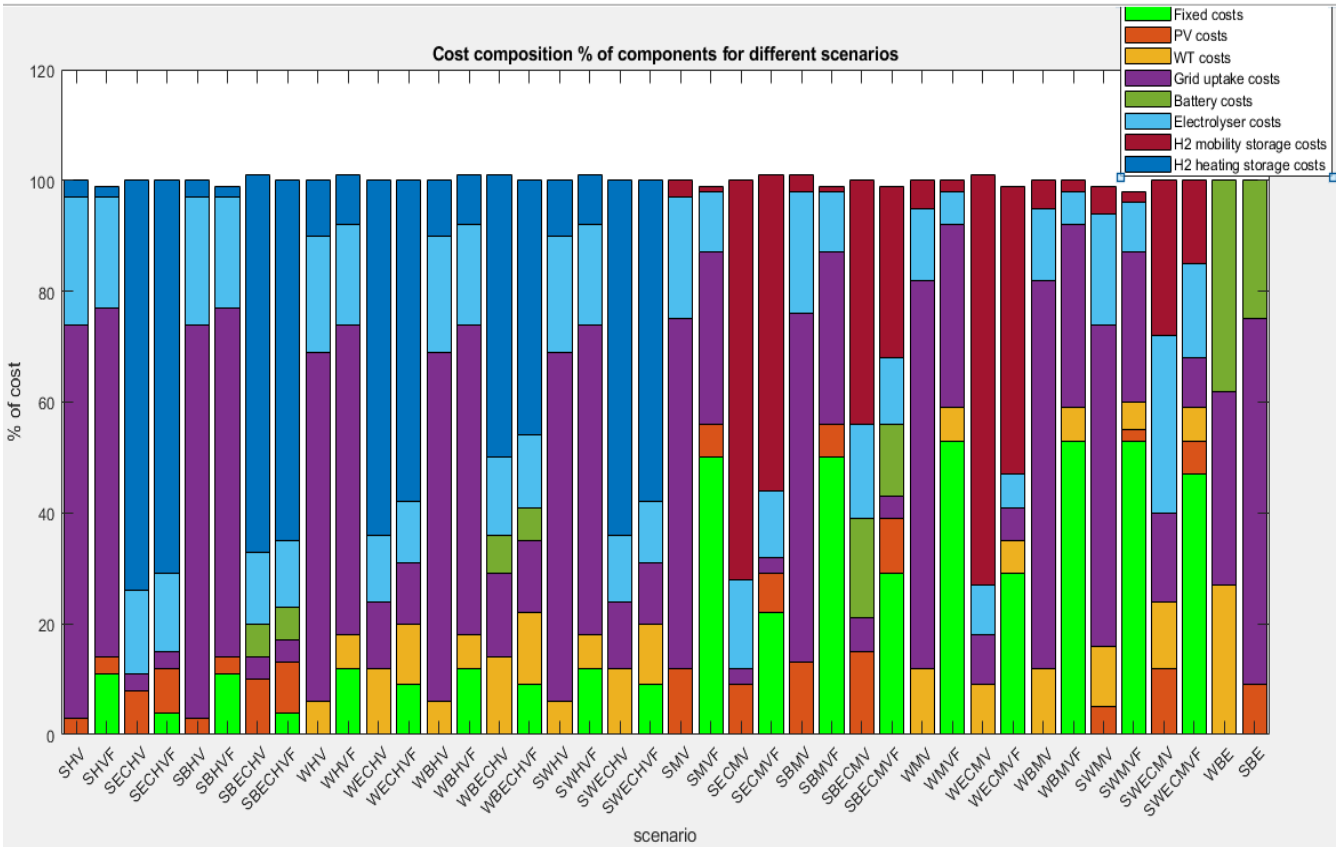

Figure 17: Cost composition percentage of total cost of components for different scenarios. Some bars do not reach 100% due to rounding off the percentages.

Effect of component deployment on cost and configuration

Observations apparent from Figure 16 and 17 and table 5 based on all scenarios:
For all systems there is a preference to use primarily grid electricity if the option is available. If no emission constraint is applied, all of the systems will have primarily grid uptake. Battery storage is not used for any of these scenarios, which is logical seeing there is an efficiency penalty by using the battery. Also the battery has no use if there is dispatchable power at any instant.

In the case of emission constraints, hydrogen storage has a positive effect for all configurations, lowering the cost of energy. For all configurations, wind seems to lead to lower costs compared to solar. The emission constraint scenarios are all more expensive than their counterpart. The effect of the emission constraint on cost is less for a combined wind and solar generation system than each one of these in isolation. Thus there seems to be a synergy effect when using both sources. This is especially apparent for the mobility supply chain comparing the emission constraint cost for solar, wind and combined wind and solar without battery. The cost effect of the wind configurations is due to a combination of wind being cheaper than solar with regards to the parameters and data used for the model, but also the fact that the emission constraint parameter for wind is lower than solar. This means that more grid electricity can also be used for these configurations, and with grid electricity being the cheapest option most of the time, lowering the price.

The fixed costs of the mobility supply chain are significantly more than the heating supply chain fixed costs and a significant portion of the total costs of the mobility supply chain.

From Figure 17 and Table 5 the following observations are apparent:
For non emission constraint scenarios, grid uptake is comfortably the highest contributor for variable cost. Applying the emission constraint lowers the grid uptake while increasing renewable electricity generator size and significantly increasing the hydrogen storage capacity for all configurations. Hydrogen storage also becomes the biggest contributor to variable cost for most scenarios. The change in installed capacity for the electrolyser is more varied, with the capacity increasing in all solar scenarios when the emission constraint is applied. Introducing a battery lowers the extent to which the electrolyser capacity is increased, but it is still significantly more than the non emission constraint scenario. Inclusion of a battery also lowers the hydrogen storage capacity needed compared to scenarios without the battery for solar and wind scenarios. For wind, the electrolyser capacity decreases with the emission constraint for the heating supply chain, albeit not by much. While the opposite happens for the mobility supply chain, where the increase is more apparent. The combined wind and solar scenarios show the same pattern, with the heating scenario including only wind. The increase in storage of all emission constraint scenarios is probably due to the intermittent nature of renewable generation requiring more storage to meet the demand. While the increase/decrease in electrolyser capacity is probably due to how the generation lines up with the demand pattern.

The electricity demand optimizations are done to see how the renewable generation uptake compares with grid electricity uptake. The electricity demand optimizations still have a significant grid uptake even though the only way of using grid electricity is through the battery and thus the efficiency penalty. This shows how grid biased the system is. But the prices are still comparable/cheaper than the grid only price (13 €ct/kWh for wind and 20 €ct/kWh for solar). This indicates that the renewable generation can compete with the grid electricity in terms of price, especially wind up to a certain uptake. But it is still cheaper to take grid energy through the battery instead of deploying more renewables with a larger battery.

Comparison of calculated cost to other models
To compare this models result with others from literature the best cost figures for the performed optimizations are used for scenarios with and without emission constraint. For heating this would be 54 and 71 €ct/kWh H_2 which converts to 21.3 (W-H scenario) and 28 (W-B-EC-H scenario) €/kg H_2 respectively. See table 5 for the component sizes of this system. For mobility this would be 77 and 87 €ct/kWh H_2 which converts to 30.3 (S-W-M scenario) and 34.3 (S-W-EC-M scenario) €/kg H_2 respectively. See table 5 for the component sizes of this system.

Scaling the refueling station cost
In order to remove the overbuild refueling station effect, the fraction of fixed costs that causes this effect is transformed into the cost if the station is build for 300 kg/day capacity. For the used scenarios these fixed costs contribute to 50 and 44% of the fixed cost effect. The computation is (0.771-0.354)*0.5/7.5 + 0.5*(0.771-0.354) + 0.354 = 59 €ct/kWh H_2 and 71 €ct/kWh H_2 using the same computation but with different data. This translates to 23.3 (S-W-M scenario) and 28 (S-W-EC-M) €/kg H_2. Thus, the overcapacity of the refueling station for this low demand increases the cost by 30.6 and 22.5% for no EC and with EC.

Hydrogen for heating cost comparison
The price of hydrogen for heating is much higher in the results of this study compared to previous research. The model of Hogewerf [15] resulted in a price of 6.39 €/kg compared to 21.3 (no EC) and 28 (EC) of this study. The cost parameters and modelling approach of his work was very different from this study. He used a fixed grid electricity price that was more than twice of the one used in this study and the solar electricity price was very low. These two choices are the exact opposite of the emergent behavior apparent in this model, as the grid uptake is heavily favored, and solar energy use leads to higher prices. The cost of solar is determined by the weather data and other cost parameters and is not a certain cost parameter. It is likely that the big difference is due to the previously mentioned difference in cost parameters used. The assumptions taken by Hogewerf may very well be true in the future if carbon pricing is introduced, and thus increasing a largely fossil generated grid electricity price. Also, further technological development may lead to declining solar prices leading to the cost parameter used, but currently this cannot be true, or PV deployment would be much higher. This model also incorporates the heating network fixed cost which Hogewerf did not implement. Hogewerf also reviewed other research and the cost of hydrogen reported in these studies falls between 0.94 to 20 €/kg [15]. Most of the studies fall in the middle of this range at around 6-10 €/kg, thus close to the value determined by Hogewerf. Based on these values, it seems that this model is more on the conservative side regarding hydrogen cost compared to other work, although no emotion was involved in making modelling choices. The apparent outcome is that there is still much room for cost reductions before hydrogen becomes competitive compared to conventional technologies with the data used.

Hydrogen for mobility cost comparison
The hydrogen for mobility cost was compared to different previous studies mentioned in the following review [84]. The price of hydrogen mentioned in this review varied in the range 3.2-29.7 €/kg, with the highest cost of onsite hydrogen production coming from onsite electrolysis. The cost is also mentioned to be largely dependent on the size of the refueling station and the share of FCEV in the vehicle fleet. In this work the assumption is taken that every household considered in the project uses this station for refueling, thus the share of FCEV in the vehicle fleet is automatically high. The cost is also calculated for the overbuild refueling station and the scaled refueling station. Just like the heating supply chain it seems this model tends to calculate a cost on the higher end of previous studies for hydrogen, with the overbuild station cost 30.3 (no EC) and 34.3 (EC) €/kg H_2 being slightly higher and the scaled station cost 23.325 (no EC) and 28 (EC) €/kg H_2 being

slightly lower than the highest cost reported in the review of 29.7 €/kg. It must be noted that not all configurations were optimized, thus one of the more complex configurations could still lower the cost. Also performing sensitivity analysis could indicate parameters that contribute the most to cost and thus be more likely to cause errors in the results. The same statement as for the heating case is apparent here, with much cost reductions being needed before hydrogen becomes competitive with conventional technologies in regards with the data used.

As for the developed model, it was used with certain input data for these calculations, but the method is versatile and can be used for systems of differing sizes and weather resource by changing the input and by having enough computational power.

Discussion and areas of improvement

The wind scenarios give lower prices compared to solar, but these results are not realistic due to using LP. The number of units are not integers and thus not possible in reality. MILP should be used to get realistic optimized scenarios. This would lead to higher prices.

The high cost of hydrogen for mobility is partly due to the fixed CAPEX/OPEX costs which are valid for a refueling station up to a capacity of 300 kg/day. The demand for which is calculated is maximum around 40 kg/day. Thus the 'capacity factor' of the considered station would be really low compared to its capabilities and thus inflating the price per unit hydrogen. The fixed costs are for a station which could have a demand around 7.5 times higher than our considered demand. Building a refueling station for such a low throughput is thus not economic.

Performing more optimizations would lead to more concrete statements made being possible, especially the optimization of combined wind and solar with battery system. Optimizations which combine demands would also be informative as to see whether these systems have some interaction effect that could lower/increase price compared to individual systems.

The bias for grid energy could be made less apparent by introducing some carbon pricing in the cost parameters, which would level the playing field for the renewable generators.

To lower optimization computational time, an option is to calculate the fraction of cost that can be attributed to one year of project time and running the optimizations over this smaller timescale. If the calculation is done properly, the results should be similar to the long time scale, if the data used is comparable. This would make performing sensitivity analysis less time consuming leading to better insights. However, some of the benefits from using longer timescales, such as more variability in operation due to changing weather patterns are lost if this smaller timescale is used. Another option is to increase the timestep of the model. This should also decrease computational time, albeit with a probable negative effect on model accuracy.
Sensitivity analysis would be interesting to see the effect of the electrolyser system efficiency on the model output. This would indicate whether the constant efficiency assumption errors present in the model significantly change the output. If the effect is large, incorporating changing system efficiencies can address this.

In the case of integrating multiple demands: to calculate the levelized cost of individual products in a system, LCOE calculations must be done that attribute the fraction of cost of the system needed to produce a unit of product. This can be done by considering the fraction of the flow of energy emerging from or flowing through a certain component that can be attributed to a certain product. These fractions become apparent by considering the energy balance over the system. The fraction of energy from a component used to produce the product can be then used in combination with the cost parameters and decision variables in a LCOE calculation. These metrics could then be used to see how a

more complex system decomposes into smaller systems. Comparisons can then be made between individual smaller systems and the decomposed system to see if synergies are formed in more complex systems which lower/increase the cost. This was not done due to lack of computational power required to preform optimisations integrating multiple demands.

The model can be expanded by including costs such as the electrical infrastructure costs. These are not included because these are assumed to be dependent on geometric distances between the components that are not known.

The wind and solar production potential calculations can be improved by more complex modelling.

5 Conclusions and recommendations

This paper covered the design and implementation of a mathematical optimization model to answer the following research question: Which component sizes lead to the lowest levelized cost of hydrogen (LCOH) for different energy system configurations and meets the various demands (hydrogen for heating, hydrogen for mobility, electricity use) and emission limits at all times? The energy system is assumed to possibly consist of the following variable size components: wind energy generators, solar energy generators, grey grid electricity, battery system, electrolyser, heating hydrogen storage, mobility hydrogen storage and fixed size components: gas receiving station, refueling compressor and hydrogen refueling station.

The developed model was used on different system configurations and with enough time calculated the optimized configuration that led to the lowest cost for a number of them. This was done on a case study concerning the Hoogeveen hydrogen project, but the model is versatile and can be used to calculate optimized scenarios for different demands and weather patterns by changing the input.

Analysis of the operational performance of one of these scenarios was consistent, showing no strange trends, thus indicating possible real-life operation. The following observations where apparent for the performed optimizations:
-All of the systems prefer grid uptake as majority of generation if no constraints are applied to the system, grid uptake portion of variable costs is also the highest for these scenarios.
-Putting an emission constraint on the system increases the price.
-Storage lowers the cost when used in emission constrained systems but at high capacities and storage also becomes the highest portion of variable cost for these scenarios.
-Solar scenarios lead to the highest costs followed by wind and combined wind and solar have the lowest costs.

The lowest costs calculated by the model for hydrogen for heating are 54 €ct/kWh and 71 €ct/kWh H_2, which converts to 21.3 €/kg (W-H scenario) and 28€/kg H_2 (W-B-EC-H scenario). The component sizes for this system are the power equivalence of 1.071 60 kW wind turbine units, 6723.79 MWh grid uptake, 7473 kWh heating storage capacity and 183 kW electrolyser capacity (W-H scenario).
And the component sizes for the other scenario are the power equivalence of 3.179 60 kW wind turbine units, 2214.7 MWh grid uptake, 177 kWh battery capacity, 166 kW electrolyser capacity and 52928 kWh hydrogen heating storage capacity (W-B-EC-H scenario).

For mobility this would be 77 and 87 €ct/kWh H_2 which converts to 30.3 (S-W-M scenario) and 34.3 (S-W-EC-M scenario) €/kg H_2.
The component sizes are 361.6 m^2 PV area, the power equivalence of 1.370 60 kW wind turbine units, 4672 MWh grid uptake, 128 kW electrolyser capacity and 1007.7 kWh mobility storage capacity (S-W-M scenario).
For the other system the power equivalence of 1.771 60 kW wind turbine units, 1077 m^2 PV area, 1744.65 MWh grid energy uptake, 258 kW electrolyser capacity and 6930.9 kWh mobility storage capacity (S-W-EC-M scenario).
In order to remove the overbuild station effect, the fraction of fixed costs that causes this effect is transformed into the cost if the station is built for 300 kg/day capacity. This leads to costs of 23.3 (S-W-M scenario) and 28 (S-W-EC-M scenario) €/kg H_2. Thus, the overcapacity of the refueling station for this low demand increases the cost by 30.6 and 22.5%.

Previous literature gives costs of hydrogen production ranging 0.94 to 20 €/kg for heating and ranging 3.2-29.7 €/kg for mobility. The costs determined by this model are on the

higher end of this range and do not seem extreme, indicating much cost reductions being needed before hydrogen becomes competitive with conventional technologies in regards with the data used.

There are areas for improvement in the model which can be addressed in future work. These include improving the solar and wind power potential calculations for the input, including a varying or constrained electrolyser system efficiency instead of using a fixed value, using MILP to get realistic unit values in the case of wind turbines, introducing carbon pricing so that the model is not as heavily grid biased, performing more complex system configuration optimizations and sensitivity analysis on the parameters. Some of these areas were planned for this study but long computational times made it infeasible. In order to lower computational time, the model costs over project lifetime can be calculated to 1 year or the temporal resolution can be decreased. This would have benefits in terms of computation time, but the option of including operational variability over years would be lost.

References

[1] IPCC , "Climate Change 2014 Synthesis Report Summary for Policymakers," IPCC, Geneva , 2014.

[2] L. Li, H. Manier and M. Manier, "Hydrogen supply chain network design: An optimization-oriented review," *Renewable and Sustainable Energy Reviews,* vol. 103, pp. 342-360, 2019.

[3] A. Almansoori and N. Shah, "Design and operation of a future hydrogen supply chain: Snapshot Model," *Chemical Engineering Research and Design,* vol. 84, p. 423–438, 2006.

[4] A. Almansoori and N. Shah, "Design and operation of a future hydrogen supply chain: Multi-period model," *international journal of hy drogen energy,* no. 34, p. 7883–7897, 2009.

[5] A. Almansoori and N. Shah, "Design and operation of a stochastic hydrogen supply chain network under demand uncertainty," *International Journal of Hydrogen Energy ,* no. 37, pp. 3965-3977, 2012.

[6] P. Nunes, F. Oliveira, S. Hamacher and A. Almansoori, "Design of a hydrogen supply chain with uncertainty," *International Journal of Hydrogen Energy ,* pp. 1-11, 2015.

[7] S. Han and J. Kim, "A multi-period MILP model for the investment and design planning of a national-level complex renewable energy supply system," *Renewable Energy,* vol. 141, pp. 736-750, 2019.

[8] S. Samsatli and N. Samsatli, "A general spatio-temporal model of energy systems with a detailed account of transport and storage," *Computers and Chemical Engineering,* no. 80, pp. 155-176, 2015.

[9] L. Welder, D. Severin Ryberg, L. Kotzur, T. Grube, M. Robinius and D. Stolten, "Spatio-Temporal Optimization of a Future Energy System for Power-to-Hydrogen Applications in Germany," *Energy ,* vol. 158, pp. 1130-1149, 2018.

[10] L. Li, H. Manier and M. Manier, "Integrated optimization model for hydrogen supply chain network design and hydrogen fueling station planning," *Computers and Chemical Engineering,* vol. 134, pp. 1-28, 2019.

[11] C. Clack, Y. Xie and A. MacDonald, "Linear programming techniques for developing an optimal electrical system including high-voltage direct-current transmission and storage," *Electrical Power and Energy Systems ,* vol. 68, pp. 103-114, 2015.

[12] M. Fripp, "https://pubs.acs.org," 30 March 2012. [Online]. Available: https://pubs.acs.org/doi/10.1021/es204645c. [Accessed 16 September 2020].

[13] T. Lambert, P. Gilman and P. Lilienthal, "Micropower System Modeling With HOMER," in *Integration Of Alternative Sources Of Energy*, Hoboken, John Wiley & Sons, 2006, pp. 379-418.

[14] X. De La Cruz, L. Viola, T. Ohishi and L. da Silva, "Optimal Scheduling of Grid-Connected Microgrids with Different Intermittent Renewable Generation," in *2019 IEEE PES Innovative Smart Grid Technologies Conference - Latin America (ISGT Latin America)*, Gramado, 2019.

[15] B. Hogewerf, "Optimization of a hydrogen supply chain for heating in a residential area: A minimization of costs," HUAS, Groningen , 2020.

[16] J. Aué, T. van der Meij, E. J. Hengeveld, D. Tempelman, B. Meijer, K. Boer, W. Hazenberg, J. Teerling, J. Pereboom and W. Elving, "Waterstofwijk Plan voor waterstof in Hoogeveen," Project consortium Waterstofwijk Hoogeveen, 2020.

[17] E. Hecht and J. Pratt, "Comparison of conventional vs. modular hydrogen refueling stations, and on-site production vs. delivery," Sandia National Laboratories, Albuquerque/Livermore, 2017.

[18] E. Skoplaki and J. Palyvos, "On the temperature dependence of photovoltaic module electrical performance: A review of efficiency/power correlations," *Solar Energy,* vol. 83, pp. 614-624, 2009.

[19] C. Honsberg and S. Bowden, "https://www.pveducation.org," [Online]. Available: https://www.pveducation.org/pvcdrom/properties-of-sunlight/solar-radiation-on-a-tilted-surface. [Accessed 25 October 2020].

[20] KNMI, "https://www.knmi.nl," KNMI, [Online]. Available: https://www.knmi.nl/nederland-nu/klimatologie/uurgegevens. [Accessed 22 November 2020].

[21] KNMI, "http://projects.knmi.nl/," [Online]. Available: http://projects.knmi.nl/klimatologie/metadata/hoogeveen.html. [Accessed 22 November 2020].

[22] W. van Sark, L. Bosselaar and P. Gerissen, "Update of the Dutch PV specific yield for determination of PV contribution to renewable energy production: 25% more energy!," in *29th European Photovoltaic Solar Energy Conference and Exhibition*, Amsterdam, 2014.

[23] Fraunhofer Institute for Solar Energy Systems, "PHOTOVOLTAICS REPORT," Fraunhofer Institute for Solar Energy Systems, Freiburg , 2020.

[24] Astronergy, "http://www.astronergy.com/," [Online]. Available: http://www.astronergy.com/attch/download/20160214%20EN%20ASM6612P.pdf. [Accessed 22 November 2020].

[25] Astronergy, "https://documents.unboundsolar.com," [Online]. Available: https://documents.unboundsolar.com/media/astronergy-chsm6612p-305-solar-panel-specs-138519736.pdf. [Accessed 22 November 2020].

[26] Astronergy, "https://www.zonnepanelen.net," [Online]. Available: https://www.zonnepanelen.net/nl/pdf/panels/astronergy-asm6610p-250-3.pdf. [Accessed 22 November 2020].

[27] BISOL, "https://www.platendt.nl," [Online]. Available: https://www.platendt.nl/pdf/bisol-0906-en.pdf. [Accessed 22 November 2020].

[28] W. Won, H. Kwon, J. Han and J. Kim, "Design and operation of renewable energy sources based hydrogen supply system: Technology integration and optimization," *Renewable Energy ,* no. 103, pp. 226-238, 2017.

[29] A. Mermoud, "https://energy.sandia.gov/," [Online]. Available: https://energy.sandia.gov/wp-content/gallery/uploads/Mermoud_PVSyst_Thu-840-am.pdf. [Accessed 22 November 2020].

[30] M. Rezaei, M. Salimi, M. Momeni and A. Mostafaeipour, "Investigation of the socio-economic feasibility of installing wind turbines to produce hydrogen: Case study," *International Journal of Hydrogen Energy,* vol. 43, no. 52, pp. 23135-23147, 2018.

[31] D. Bratton and C. Womeldorf, "The wind shear exponent: comparing measured against simulated values and analyzing the phenomena that affect the wind shear," in *Proceedings of the ASME 2011 5th International Conference on Energy Sustainability*, Washington, 2011.

[32] F. Montealegre and S. Boutsikoudi, "Wind resource assessment and yield prediction Post construction analysis Hoevensche Beemden, Laakse Vaart, Zwartenbergseweg," ECOFYS Netherlands B.V., Utrecht, 2014.

[33] Rendo Netwerken, "https://www.rendonetwerken.nl," Rendo Netwerken, 3 November 2020. [Online]. Available: https://www.rendonetwerken.nl/thuis/meter-meterstanden/#enkel-dubbeltarief. [Accessed 3 November 2020].

[34] consumentenbond.nl, "consumentenbon.nl," 23 September 2020. [Online]. Available: https://www.consumentenbond.nl/energie-vergelijken/kwh-prijs#:~:text=De%20kosten%20per%20verbruikte%20kWh,n%207%20cent%20inclusief%20btw.. [Accessed 16 December 2020].

[35] "www.alle-energieleveranciers.nl," [Online]. Available: http://www.alle-energieleveranciers.nl/p/469/tarieven-delta/. [Accessed 16 December 2020].

[36] J. Bekkering, K. Zwart, G. Martinus, J. Langerak, J. Tideman, T. van der Meij, K. Alberts, M. van Steenis and J. Nap, "Farm-scale bio-power-to-methane: Comparative analyses of economic and environmental feasibility," *International Journal of Energy Research ,* pp. 1-14, 2019.

[37] European Comission , "DIRECTIVE (EU) 2018/2001 OF THE EUROPEAN PARLIAMENT AND OF THE COUNCIL of 11 December 2018 on the promotion of the use of energy from renewable sources," Official Journal of the European Union, 2018.

[38] J. Giuntolli, A. Agostini, R. Edwards and L. Marelli, "Solid and gaseous bioenergy pathways: input values and GHG emissions. Calculated According to the Methodology Set in COM(2016) 767," Publications office of the European Union, Luxembourg , 2017.

[39] R. Edwards, J.-F. Larive, D. Rickeard and W. Weindorf, "WELL-TO-TANK (WTT) report. Version 4.a Well-to-Wheels analysis of future automotive fuels and powertrains in the European context," Publications office of the European Union, Luxembourg , 2014.

[40] N. Amponsah, M. Troldberg, B. Kington, I. Aalders and R. Hough, "Greenhouse gas emissions from renewable energy sources: A review of lifecycle considerations," *Renewable and Sustainable Energy Reviews,* no. 39, pp. 461-475, 2014.

[41] H. Gelani, F. Dastgeer, K. Siraj, M. Nasir, K. Niazi and Y. Yang, "Efficiency Comparison of AC and DC Distribution Networks for Modern Residential Localities," *Applied Sciences ,* vol. 9, no. 3, 2019.

[42] O. Esan, X. Shi, Z. Pan, X. Huo, L. An and T. Zhao, "Modeling and Simulation of Flow Batteries," *Advanced Energy Materials,* 2020.

[43] S. Wenham, M. Green, M. Watt and R. Corkish, "Stand-alone photovoltaic system components," in *Applied Photovoltaics*, London, Earthscan, 2007, p. 107.

[44] B. Turker, S. Arroyo Klein, E.-M. Hammer, B. Lenz and L. Komsiyska, "Modeling a vanadium redox flow battery system for large scale applications," *Energy Conversion and Management,* vol. 66, pp. 26-32, 2013.

[45] J. Platt, J. Pritchard and D. Bryant, "https://papers.ssrn.com," 8 August 2017. [Online]. Available: https://papers.ssrn.com/sol3/Delivery.cfm/SSRN_ID3015424_code2651515.pdf?abstractid=3015424&mirid=1. [Accessed 27 October 2020].

[46] D. Nguyen and L. Le, "Optimal Bidding Strategy for Microgrids Considering Renewable Energy and Building Thermal Dynamics," *IEEE Transactions on Smart Grid,* vol. 5, no. 4, pp. 1608-1620, 2014.

[47] Y. Yang, A. Li, J. Ma, N. Liu, Q. Wang and T. Du, "Research on performance of vanadium redox flow battery stack," in *IOP Conference Series: Materials Science and Engineering*, Wuhan, 2019.

[48] United Nations Industrial Development Organization, "http://www.unido.or.jp/," United Nations Industrial Development Organization, [Online]. Available: http://www.unido.or.jp/en/technology_db/2984/. [Accessed 23 November 2020].

[49] D. Bryans, V. Amstutz, H. Girault and L. Berlouis, "Characterisation of a 200 kW/400 kWh Vanadium Redox Flow Battery," *batteries ,* vol. 4, no. 54, 2018.

[50] J. Mergel, D. Fritz and M. Carmo, "Stack Technology for PEM Electrolysis," in *Hydrogen Science and Engineering Materials, Processes, Systems and Technology* , Weinheim, Wiley-VCH, 2016, pp. 331-356.

[51] S. Seyyedeh-Barhagh, M. Majidi, S. Novajan and K. Zare, "Optimal Scheduling of Hydrogen Storage under Economic and Environmental Priorities in the Presence of Renewable Units and Demand Response," *Sustainable Cities and Society ,* no. 46, 2019.

[52] G. Tjarks, J. Mergel and D. Stolten, "Dynamic Operation of Electrolyzers – Systems Design and Operating Strategies," in *Hydrogen Science and Engineering Materials, Processes, Systems and Technology*, Weinheim, Wiley-VCH, 2016, pp. 309-329.

[53] Z. Zhang, J. Zhou, Z. Zong, Q. Chen and P. Zhang, "Development and modelling of a novel electricity hydrogen energy system based on reversible solid oxide cells and power to gas technology," *International Journal of Hydrogen Energy ,* no. 44, pp. 28305-28315, 2019.

[54] A. Buttler and H. Spliethoff, "Current status of water electrolysis for energy storage, grid balancing and sector coupling via power-to-gas and power-to-liquids: A review," *Renewable and Sustainable Energy Reviews ,* no. 82, pp. 2440-2454, 2018.

[55] H. Miland, "Operational experience and control strategies for a stand-alone power system based on renewable energy and hydrogen," Norwegian University of Science and Technology, Trondheim, 2005.

[56] R. Moradi and K. Groth, "Hydrogen storage and delivery: Review of the state of the art technologies and risk and reliability analysis," *International Journal of Hydrogen Energy ,* vol. 44, pp. 12254-12269, 2019.

[57] V. Tietze and D. Stolten, "Thermodynamics of Pressurized Gas Storage," in *Hydrogen Science and Engineering Materials, Processes, Systems and Technology* , Weinheim, Wiley-VCH, 2016, pp. 601-628.

[58] F. Maslan and T. Littman, "Compressibility Chart for Hydrogen and Inert Gases," *Industrial & Engineering Chemistry,* vol. 45, no. 7, pp. 1566-1568, 1953.

[59] NREL, "https://www.nrel.gov/," 15 July 2020. [Online]. Available: https://www.nrel.gov/docs/fy20osti/77368.pdf. [Accessed 14 November 2020].

[60] K. Reddi, A. Elgowainy, N. Rustagi and E. Gupta, "Impact of hydrogen refueling configurations and market parameters on the refueling cost of hydrogen," *International Journal of Hydrogen Energy ,* vol. 42, no. 34, pp. 21855-21865, 2017.

[61] P. Schnell, "Refueling Station Layout," in *Hydrogen Science and Engineering Materials, Processes, Systems and Technology* , Weinheim, Wiley-VCH, 2016, pp. 891-914.

[62] C. v. Someren, Personal communication with Christian van Someren.

[63] Essent , "Essent.nl," [Online]. Available: https://www.essent.nl/kennisbank/energie-besparen/zelfvoorzienend-leven/nul-op-de-meter-woning. [Accessed 9 November 2020].

[64] CBS, "Transport en mobiliteit," Centraal Bureau voor de Statistiek, Den Haag, 2016.

[65] Oak Ridge National Laboratory, "fueleconomy.gov," United states Deparment Of Energy , [Online]. Available: https://www.fueleconomy.gov/feg/fcv_sbs.shtml. [Accessed 27 October 2020].

[66] M. Mintz, A. Elgowainy and M. Gardiner, "Rethinking Hydrogen Fueling: Insights from Delivery Modeling," *Transportation Research Record Journal of the Transportation Research Board,* vol. 2139, pp. 46-54, 2009.

[67] A. Jager-Waldau, "PV Status Report 2019," Publications Office of the European Union, Luxembourg, 2019.

[68] CE Delft, "Kosten zontoepassingen Methode om private en maatschappelijke kosten te vergelijken," CE Delft, Delft, 2020.

[69] Solar Bankability , "Best Practice Guidelines for PV Cost Calculation Accounting for Technical Risks and Assumptions in PV LCOE," Solar Bankability , 2016.

[70] Fraunhofer Institute For Solar Energy Systems ISE, "Levelized cost of electricity renewable energy technologies," Fraunhofer Institute For Solar Energy Systems ISE, Freiburg, 2018.

[71] K. Mongird, V. Viswanathan, P. Balducci, J. Alam, V. Fotedar, V. Koritarov and Hadjerioua, "An Evaluation of Energy Storage Cost and Performance Characteristics," *Energies ,* vol. 13, no. 3307, 2020.

[72] Platte River Power Authority Technology Assessment , "Battery Energy Storage," Platte River Power Authority Technology Assessment , 2017.

[73] M. Resch, J. Buhler, B. Schachler, R. Kunert, A. Meier and A. Sumper, "Technical and economic comparison of grid supportive vanadium redox flow batteries for primary control reserve and community electricity storage in Germany," *International Journal of Energy Research ,* vol. 43, pp. 337-357, 2018.

[74] IRENA, "Hydrogen from renewable power: Technology outlook for the energy transition," International Renewable Energy Agency, Abu Dhabi, 2018.

[75] A. Christensen, "Assessment of Hydrogen Production Costs from Electrolysis: United States and Europe," International Council on Clean Transportation, 2020.

[76] G. Matute, J. Yusta and L. Correas, "Techno-economic modelling of water electrolysers in the range of several MW to provide grid services while generating hydrogen for different applications: A case study in Spain applied to mobility with FCEVs," *International Journal of Hydrogen Energy,* vol. 44, no. 33, pp. 17431-17442, 2019.

[77] U.S. DOE Office of Energy Efficiency & Renewable Energy , "https://www.energy.gov/," [Online]. Available: https://www.energy.gov/sites/prod/files/2015/08/f25/fcto_myrdd_delivery.pdf. [Accessed 25 November 2020].

[78] U.S. DOE Hydrogen and Fuel Cells Program Record , "https://www.hydrogen.energy.gov/," [Online]. Available: https://www.hydrogen.energy.gov/pdfs/18003_current_status_hydrogen_delivery_dispensing_costs.pdf. [Accessed 25 November 2020].

[79] U.S. DOE Energy Efficiency & Renewable Energy , "H2FIRST Reference Station Design Task Project Deliverable 2-2," U.S. DOE, 2015.

[80] Accenture, "New Value New Prospects The Future of Onshore Wind Operations and Maintenance," Accenture , 2017.

[81] M. Robinius, J. Linssen, T. Grube, M. Reuss, P. Stenzel, K. Syranidis, P. Kuckertz and D. Stolten, "Comparative Analysis of Infrastructures: Hydrogen Fueling and Electric Charging of Vehicles," Institute of Electrochemical Process Engineering , Julich, 2018.

[82] B. Steffen, "Estimating the cost of capital for renewable energy projects," *Energy Economics ,* vol. 88, 2020.

[83] California Energy Comission, "Joint Agency Staff Report on Assembly Bill 8: Assessment of Time and Cost Needed to Attain 100 Hydrogen Refueling Stations in California," California Energy Comission, 2015.

[84] D. Apostolou and G. Xydis, "A literature review on hydrogen refuelling stations and infrastructure. Current status and future prospects," *Renewable and Sustainable Energy Reviews,* vol. 113, 2019.